

Simulation-based Design Methodology for a Solar-assisted Solid Desiccant Cooling System in Hot and Humid Climates

Aditya Nibandhe

A Thesis in the Department of Building,
Civil and Environmental Engineering

Presented in the Partial Fulfillment of the Requirements for the Degree of Master
of Applied Science (Building Engineering) at

Concordia University

Montreal, Quebec, Canada

August 2020

© Aditya Nibandhe 2020

CONCORDIA UNIVERSITY
School of Graduate Studies

This is to certify that the thesis prepared by

By: Aditya Nibandhe

Entitled: Simulation-based Design Methodology for a Solar assisted Solid Desiccant Cooling System in Hot and Humid Climates

and submitted in partial fulfillment of the requirements for the degree of

Master of Applied Science (Building Engineering)

complies with the regulations of the University and meets the accepted standards with respect to originality and quality.

Signed by the final examining committee:

_____	Chair
Dr. A. Athienitis	
_____	Co-Supervisor
Dr. A. Bagchi	
_____	Co-Supervisor
Dr. B. Lee	
_____	Examiner
Dr. C. Lai	External (to program)
_____	Examiner
Dr. M. Ouf	
_____	Examiner
Dr. A. Athienitis	

Approved by _____
Dr. M. Nokken, GPD
Department of Building, Civil and Environmental Engineering

Dr. M. Debbabi, Interim Dean
Gina Cody School of Engineering and Computer Science

Date _____

Abstract

Simulation-based Design Methodology for a Solar-assisted Solid Desiccant Cooling System in Hot and Humid Climates

Aditya Nibandhe

Solar-assisted Solid Desiccant Cooling (SDC) systems are effective solutions for hot and humid climates. Unlike conventional cooling systems that cool and dehumidify simultaneously, SDC systems handle sensible and latent load separately, assuring more accessible, economical and efficient air conditioning. Air-based flat-plate Photovoltaic Thermal (PV/T) collectors can provide low-grade thermal energy for SDC operation. However, PV/T collectors optimized for increasing the outlet air temperature adversely affect the electrical performance and material integrity of the photovoltaic (PV) modules. As a result, an auxiliary heater (AH) is commonly employed to boost the outlet air temperature to the required level to support the SDC system's operation; increasing the input power requirements of the integrated system.

This research investigates a Photovoltaic Thermal Solar Air Heater (PVT-SAH) assisted Solid Desiccant Cooling (SDC) system for daytime operation in hot and humid climates. The objective of the research is to develop an integrated design methodology for the complex system.

An integrated energy model of a roof-mounted PVT-SAH assisted SDC system for an archetypical low-rise mixed-use building in India is developed. First, three configurations of the integrated system are compared and an appropriate configuration is identified. A sensitivity analysis is conducted to investigate the correlation between the design parameters and the objective functions, and specify the ranges of inputs for the optimization study. A multi-objective optimization study is conducted to investigate the design solutions that reduce the solar-assisted SDC system's reliance on auxiliary heater, and optimize the solar energy gains (electrical and thermal) for space cooling application.

The integrated system configuration with proposed modifications achieved upto 135% improvement in COP_{th} and upto 48% reduction in unmet hours over the typical system configurations. As per the sensitivity analysis, the collector area, air mass flow rate, and channel height are the most important design parameters. The optimization study results show that AH energy consumption is more sensitive to the air mass flow rate for larger collector areas. In contrast, the PV electrical energy gain is more sensitive to the collector areas.

The integrated PVT-SAH assisted SDC system shows a great potential to reduce both energy consumption and peak demand. The design methodology proposed in this study will facilitate the design and application of an integrated PVT-SAH assisted SDC system in hot and humid climates.

Acknowledgements

In the fall of 2016, I left behind the comfort and privileges of home and moved to a new country, different in many ways compared to India. It took me a while to get used to life in Canada. As a result, my first semester at Concordia University was far from ideal. In the winter of 2017, I met Dr. Lee, who noticed my potential and offered me this research opportunity. Life truly changed for the better from that point onwards, and I haven't looked back or regretted any decisions. I would like to express my utmost gratitude towards my co-supervisors, Dr. Lee and Dr. Bagchi, for their continuous support, guidance, and encouragement throughout the program. I have learned many valuable lessons about research and life itself from you. Thank you!

I would like to thank all of Dr. Lee's talented research students who have helped me in my work and shared many joyful memories outside of school. I would also like to extend my gratitude towards Dr. Reddy from the Indian Institute of Technology Madras, Dr. Athienitis, and all the people involved in our collaborative project through the IC-IMPACTS. Also, a special thanks to dear Nima and Stratos for all your efforts, insights, and contributions towards making this work better, while helping me enjoy this journey.

I would like to acknowledge the financial support from the IC-IMPACTS Research Center of Excellence and the Department of Building, Civil and Environmental Engineering at Concordia University.

I would like to thank my family and friends for their support and motivation from near and far. To my partner, Olivia, thank you for your unconditional love and support. You encourage me to become a better version of myself every day.

Shubhangi and Shridhar, my Aai and Baba, without you, none of it would have been possible. You brought me into this world, raised me to be a good human being, and mindful of my actions and intentions towards others. You have tirelessly worked all your life to offer me the best and instilling in me the confidence to give my best in life. I hope you will feel happy and satisfied watching your son accomplish one of his biggest milestones. This one goes to you.

Table of Contents

List of Figures	vii
List of Tables	viii
Nomenclature	ix
Chapter 1. Introduction.....	1
1.1 Cooling Energy Consumption in Buildings and Building-related emissions in hot and humid climates	1
1.2 Problem Statements	2
1.3 Objective	3
1.4 Thesis Outline.....	4
Chapter 2. Literature Review	5
2.1 Applications of Solar Technologies in Buildings	5
2.2 Solar-assisted Cooling Technologies.....	6
2.3 Solar-assisted Solid Desiccant Cooling (SDC) systems.....	8
2.4 Optimization of Solar-assisted SDC systems	13
2.5 Potential Areas and Scope of this Research	14
Chapter 3 Methodology	16
3.1 Integrated PVT-SAH assisted SDC system configuration	16
3.1.1 Identification and selection of solar and thermally driven cooling technologies.....	16
3.1.2 Integration of the PVT-SAH and SDC system into an appropriate configuration.....	17
3.2 Identification of Design Parameters and Formulation of Optimization Problem	19
3.3 Multi-Objective Optimization to Investigate the Design Solutions.....	19
Chapter 4 Case Study	21
4.1 Location Analysis	21
4.2 Developing of the Building Energy Model	23
4.2.1 Building Description	23
4.2.2 Weather Data	24
4.2.3 Lighting, Electric Equipment, Occupancy.....	25
4.2.4 Idealized Air Loads.....	26
4.3 Developing of the PVT-SAH assisted SDC System Model.....	26
4.3.1 Equipment Sizing for Baseline Model	28
4.3.2 PVT-SAH Description	29

4.3.3 Integrated PVT-SAH assisted SDC system Operation.....	29
4.4 Retail store operation using Different Integrated System Configurations	30
4.4.1 Configuration 1: Typical integrated PVT-SAH assisted SDC system configuration in ventilation mode (100% fresh air)	30
4.4.2 Configuration 2: Typical integrated PVT-SAH assisted SDC system configuration in recirculation mode	31
4.4.3 Configuration 3: Existing integrated PVT-SAH assisted SDC system configuration in recirculation mode with proposed modifications	31
4.5 Sensitivity Analysis and Optimization Study	32
4.5.1 Sensitivity Analysis.....	32
4.5.1 Optimization Study	33
Chapter 5. Results and Discussions.....	34
5.1 Simulation Results of the Case Study	34
5.1.1 PVT-SAH Energy Gain.....	34
5.1.2 AH Energy Consumption	36
5.1.3 Thermal Coefficient of Performance.....	37
5.1.4 Unmet Hours.....	38
5.1.5 Comparative Performance Improvement.....	39
5.2 Sensitivity Analysis Results	40
5.3 Optimization Study Results.....	41
Chapter 6. Conclusions.....	45
6.1 Contributions.....	45
6.2 Future Work Opportunities	46
References.....	47
Appendices.....	52
Appendix A.....	52
Appendix B.....	53
Appendix C	54
Appendix D.....	56

List of Figures

Figure 1 Conventional Solid Desiccant Cooling System in Ventilation Mode (Jani et al., 2016).....	9
Figure 2 Solid Desiccant Cooling System in Recirculation Mode (Jani et al., 2016)	10
Figure 3 Typical integrated PVT-SAH assisted SDC system configuration 1 (Ventilation Mode)	18
Figure 4 Typical integrated PVT-SAH assisted SDC system configuration 2 (Recirculation Mode).....	18
Figure 5 Integrated PVT-SAH assisted SDC system configuration 3 with proposed modifications (Recirculation Mode).....	18
Figure 6 Annual Global Horizontal Irradiance (GHI) in Chennai, India (Kruglov et al., 2018).....	22
Figure 7 Annual Average Air Temperature in Chennai, India (Kruglov et al., 2018).....	22
Figure 8 Monthly Profile of Average Dry Bulb Temperature in Chennai (Kruglov et al., 2018).....	22
Figure 9 Monthly Profiles of Global Horizontal and Average Cloud Cover Irradiance in Chennai (Kruglov et al., 2018)	23
Figure 10 Common Building Typologies in the state of Tamil Nadu, India (National Disaster Management Authority, 2013)	23
Figure 11 3D Rendering of the Building Model	24
Figure 12 Hourly Profile of Key Weather Data: Winter Day	25
Figure 13 Hourly Profile of Key Weather Data: Summer Day	25
Figure 14 Integrated PVT-SAH assisted SDC system configuration 3 with proposed modifications (Recirculation Mode).....	29
Figure 15 Typical integrated system configuration 1 in ventilation Mode	30
Figure 16 Typical integrated system configuration 2 in recirculation mode	31
Figure 17 Existing integrated system configuration 3 in recirculation mode with proposed modifications .	32
Figure 18 Monthly PVT-SAH Electrical Energy Gain (kWh).....	34
Figure 19 Monthly PVT-SAH Thermal Energy Gain (kWh)	35
Figure 20 Monthly Average PVT SAH Inlet Air Temperature (°C)	35
Figure 21 Monthly Average SAH Inlet and Outlet Air Temperature (°C).....	37
Figure 22 Monthly AH Energy Consumption (kWh).....	37
Figure 23 Monthly Average Thermal Coefficient of Performance (COP _{th})	38
Figure 24 Monthly Average Room Air Temperature (°C).....	39
Figure 25 Monthly Average Room Relative Humidity (%).....	39
Figure 26 Impact of Design Parameters on the Outputs	40
Figure 27 Bubble plot showing the design space for selected design parameters	42
Figure 28 Bubble plot showing the Pareto Front between the Objective functions	42
Figure 29 Parallel Plot showing variation in the objective functions for small collector areas	44
Figure 30 Parallel Plot showing variation in the objective functions for large collector areas	44
Figure 31 Comparison of Surveyed Data and Simuated Data	53
Figure 32 Psychrometric chart showing steady state operation of integarted system configuration 1	54
Figure 33 Psychrometric chart showing steady state operation of integarted system configuration 2	54
Figure 34 Psychrometric chart showing steady state operation of integarted system configuration 3	55
Figure 35 Parallel Plot with all possible integarted system designs	56
Figure 36 Parallel Plot showing variation in outputs for small collector areas	56
Figure 37 Parallel Plot showing variation in outputs for medium collector areas.....	57
Figure 38 Parallel Plot showing variation in outputs for medium collector areas.....	57
Figure 39 Parallel Plot showing variation in outputs for large collector areas	58

List of Tables

Table 1 Classification of Relevant Climate Zones	6
Table 2 Performance Overview of Solar Thermally-driven Cooling Technologies.....	8
Table 3 PV/T Performance Improvement Methods	9
Table 4 Building Envelope Properties	24
Table 5 Building Internal Gains.....	25
Table 6 Dimensions of PVT-SAH for the baseline model.....	29
Table 7 Design Parameters for the Sensitivity Analysis.....	32
Table 8 Design Parameters for optimization.....	33
Table 9 Details of Optimization	33
Table 10 Comparison of full factorial with optimization	33
Table 11 Annual PVT SAH Electrical and Thermal Energy Gains	36
Table 12 Annual AH Energy Consumption.....	37
Table 13 Unmet Hours Comparison.....	38
Table 14 Comparison of Performance Improvements.....	40
Table 15 Comparison of Surveyed Data and Simulated Data.....	53

Nomenclature

Symbols	Definition
β_{PV}	Temperature coefficient of the module
COP_{th}	Thermal coefficient of performance of the SDC system
C_p	Specific heat of air (J/kg°C)
D_{Hi}	Hydraulic diameter (m)
ϵ	direct evaporative cooler saturation efficiency (effectiveness)
f_i	Friction factor
h_{HX}	Enthalpy of air at the outlet of the heat exchanger (kJ/kg)
h_{supply}	Supply air enthalpy (kJ/kg)
h_{reg}	Regeneration air enthalpy (kJ/kg)
h_{room}	Room air enthalpy (kJ/kg)
h_{top}	Top convective heat transfer coefficient
L_i	Length of the air channel (m)
\dot{m}	Mass flow rate of air (kg/s)
\dot{m}_{supply}	Supply air mass flowrate (kg/s)
\dot{m}_{return}	Return air mass flowrate (kg/s)
η_{deh}	Dehumidification efficiency (%)
η_{fan}	Fan efficiency (%)
η_{motor}	Motor efficiency (%)
η_{PV}	Pv electrical efficiency (%)
η_{STC}	Pv electrical efficiency under standard conditions (%)
ΔP_f	Frictional pressure drop (Pa)
ΔP_k	Kinetic pressure drop (Pa)
ΔP_m	Minor frictional pressure drop (Pa)
ΔP_M	Major frictional pressure drop (Pa)
Q_{air}	Thermal energy extracted by the circulating air (W)
q_{cool}	Cooling energy supplied
q_{heat}	Heating energy required
ρ	Density of air (kg/m ³)
T	Temperature (°C)
$T_{in,db}$	Incoming air dry bulb temperature (°C)
$T_{in,wb}$	incoming air wet bulb temperature (°C)
$T_{out,db}$	outgoing air dry bulb temperature (supply air) (°C)
T_o	Temperature of air at the outlet of pvt-sah (°C)
T_i	Temperature of air at the inlet of pvt-sah (°C)
T_{PV}	PV temperature
T_{STC}	PV Module Surface Temperature (25°C)
\dot{V}	Volumetric flow rate (m ³ /s)
V_{iavg}	Average air velocity through the air channel (m/s)
V_{wind}	Wind velocity at reference height (m/s)
w_{amb}	ambient air specific humidity (g/kg of dry air)
w_{ideal}	ideal specific humidity (g/kg of dry air)

$w_{process DW out}$	process air specific humidity at the desiccant wheel outlet (g/kg of dry air)
\dot{W}_{fan}	Electrical fan power (kW)
\dot{W}_h	Hydraulic fan power (kW)

Acronyms	Definition
ACH	Air changes per hour
AH	Auxiliary heater
ANOVA	Analysis of Variance
ASHRAE	American Society of Heating, Refrigeration and Air Conditioning Engineers
BAPV	Building Applied Photovoltaics
BEE	Bureau of Energy Efficiency
BIPV	Building Integrated Photovoltaic
BIS	Bureau of Indian Standards
CDD	Cooling Degree Days
COP	Coefficient of Performance
DBT	Dry Bulb Temperature
DEC	Direct Evaporative Cooling
DINC	Direct Indirect Evaporative Cooling
DW	Desiccant Wheel
EPI	Energy Performance Index
GHG	Green House Gases
GHI	Global Horizontal Irradiance
HVAC	Heating, Ventilation, And Air Conditioning
IEA	International Energy Agency
IEC	Indirect Evaporative Cooling
MOGA	Multi-Objective Genetic Algorithm
NBC	National Building Code
NZEB	Net Zero Energy Building
PV	Photovoltaic
PVT	Photovoltaic Thermal
RES	Renewable Energy Sources
RH	Relative Humidity
SAH	Solar Air Heater
SDC	Solid Desiccant Cooling
SF	Solar Fraction
SHGC	Solar Heat Gain Coefficient
SW	Sensible Wheel
TMY	Typical Meteorological Year
TW	Thermal Wheel
UTC	Unglazed Transpired Collector
VCR	Vapor Compression Refrigeration
VLT	Visible Light Transmittance

Chapter 1. Introduction

1.1 Cooling Energy Consumption in Buildings and Building-related emissions in hot and humid climates

Buildings account for one-third of the world's final energy consumption, the highest share among all the sectors (Global Alliance for Buildings and Construction, 2016) (IEA, 2019c). Also, around 28% of the total energy-related CO₂ emissions (IEA, 2019b) and 20% of the GHG emissions are building-related (Global Alliance for Buildings and Construction, 2016). Although building energy use intensity per square meter improved, the CO₂ emissions increased by more than 25% since 2000 (IEA, 2019b). Most of the growing countries are from Asia, Africa, and the middle east with rapid development, especially in the building sector. A steady rise in cooling energy demand associated with buildings is expected, especially for locations with hotter climates (IEA, 2019a) (Global Alliance for Buildings and Construction, 2016). Space cooling is an important reason for the rise in building-related CO₂ and GHG emissions (IEA, 2019b) (Global Alliance for Buildings and Construction, 2016). Cooling energy demand in buildings has more than doubled between 2000 and 2017 (IEA, 2019b), making it the main driver for energy demand and fastest-growing end-use in the building sector (Global Alliance for Buildings and Construction, 2016) (International Energy Agency, 2019) (IEA, 2018). If the trend continues, without any further efficiency gains, cooling energy demand will continue to rise and will be doubled by 2040 (IEA, 2019b).

Space cooling accounted for 10% of total electricity demand averaged across all countries in 2016 (IEA, 2018). However, in some countries with hotter climates, space cooling can account for a consistent share of total electricity demand throughout the year. It can almost be doubled during the summer months. In some countries characterized by very hot summers, space cooling demand accounts for almost half of the total electricity demand during summertime. High ambient temperatures can also affect electricity networks, as high demand and high temperatures can heat up power lines impairing their performance (IEA, 2018). Cooling demand jumps during hot ambient conditions, increasing the peak load and putting more stress on the power grid. In such hot conditions, the power grid's reliability can be undermined because of hot equipment that can result in outages (IEA, 2018).

Currently, space cooling demand in buildings is most commonly fulfilled by Vapor Compression Refrigeration (VCR) based air conditioning systems. VCR systems are one of the main contributors to building energy demand, especially in hot and humid climates. Cooling technologies such as Vapor Compression Refrigeration (VCR) system is widely used for space cooling in buildings. While handling air with high moisture content, a VCR system ends up cooling the air beyond the required setpoint temperature to achieve dehumidification, making the VCR system's operation in hot and humid climates energy-intensive and inefficient. The increase in summertime peak cooling demand of buildings also increases the peak load as well as total annual energy consumption because of the VCR system; placing additional stress on the electrical grid (Guo et al., 2017) and indirectly increasing the CO₂ and GHG emissions (IEA, 2018). VCR systems

themselves are not responsible for CO₂ and GHG emissions unless there is a leakage. However, VCR systems are responsible for increased summertime peak demand and annual energy consumption. The generation of electricity needed to sustain the VCR systems' operation accounts for a sizeable increase in CO₂ and GHG emissions (IEA, 2018).

On-site energy generation using Renewable Energy Sources (RES) is a great way to alleviate the stress on the power grid. Fortunately, the peak cooling demand occurs during the daytime, which coincides with peak solar irradiance, making solar cooling technologies a suitable choice. Solar technologies mostly dominate on-site energy generation because it can be easily integrated and is economical at the building level. Also, recently, clean energy technology like a thermally-driven cooling system has been proposed as an alternative to the VCR system. This is largely because thermally-driven cooling systems use waste heat or solar thermal heat as input energy instead of electricity. On-site application of PV/T collectors in space cooling has been an important topic of discussion. Liquid or air-based photovoltaic thermal (PV/T) collectors can be used, especially in the building's façade or rooftop to produce electricity and useful heat. This helps to overcome the limitation of overheating of PV modules as well as provides useful thermal energy. In hot climates, liquid-based solar technologies are primarily deployed for electricity production, domestic hot water and thermal storage applications. Whereas, in cold climates, air-based solar technologies are predominantly used for application in Heating, Ventilation and Air-Conditioning (HVAC) systems in buildings. This study will focus on the space cooling application of air-based roof PVT collectors using a thermally-driven cooling system.

1.2 Problem Statements

In order to cover buildings' air-conditioning demand, both electrically and thermally operated cooling systems are available in the market. Conventional air conditioning technology is dominated by Vapor Compression Refrigeration (VCR) systems. Such a system relies on the phase change property of certain liquids called refrigerants to provide cooling on the evaporator side and heating on the condenser side (IEA, 2018). VCR systems have been in the market for a long time now, making these machines very economical and readily available in almost any size globally (IEA, 2018). Commonly used cooling technologies handle sensible and latent loads together. Dehumidification in these systems is achieved by cooling the air below its dew point, which results in condensing of the moisture and eventually providing the desired degree of dehumidification (Ahmed et al., 2005). However, this process of dehumidification often leaves the supply air cooled beyond the required room setpoint (Ahmed et al., 2005), making the system energy-intensive and inefficient when handling air with high moisture content (Fan et al., 2019)(Jani et al., 2016). The increase in summertime peak cooling demand of buildings also increases the peak load as well as total annual energy consumption because of the VCR system, placing additional stress on the electrical grid (Guo et al., 2017), and indirectly increasing the CO₂ and GHG emissions (IEA, 2018).

Commonly used cooling technologies in buildings are energy-intensive and, therefore inefficient when handling air with high moisture content, consequently increasing the peak load and total annual energy consumption and indirectly increasing the emissions.

Alternatively, clean energy technology, such as thermally driven cooling systems assure more accessible, economical and efficient air conditioning in hot and humid climates, as a Solid Desiccant Cooling (SDC) system, for instance, handles the sensible and latent load separately while using thermal energy as input instead of electricity (Jani et al., 2016). In an SDC system, a desiccant material dehumidifies the supply air and an evaporative cooler helps to provide required air cooling. This way a thermally driven SDC system operates to deal with the latent and sensible load separately to provide the air-conditioning like conventional cooling systems but requires less electricity. An SDC system can operate using the thermal energy available from industrial/other waste heat or solar heat sources. Usually, SDC systems need air temperatures in the range on 50-80°C to regenerate the desiccant wheel to ensure continuous operation although in extremely humid climates higher regeneration temperatures are required (Ge et al., 2014)(H. Li et al., 2011)(Gommed & Grossman, 2007)(Jani et al., 2016).

Assuming daytime operation, a PV/T collector coupled with an SDC system can provide air conditioning and electricity to partially offset the peak load on the grid (Fan et al., 2019). Among the liquid-based (water) and air-based solar PV/T technologies, the water-based technologies certainly have a significant advantage over the air in terms of heat transfer and thermal storage capacity. In contrast, the air-based technologies benefit from no leakage, lower weight of the entire assembly, lower initial costs, and lower maintenance costs and effort (Yang & Athienitis, 2016).

It is expected that an air-based PVT collector will have to maintain a high outlet air temperature to drive an SDC system. However PV/T collectors optimized for increasing the outlet air temperature adversely affect the electrical performance and material integrity of the PV modules (Yang & Athienitis, 2016). As a result, an auxiliary heater (AH) is commonly employed to boost the outlet air temperature to the required level to support the SDC system's operation; increasing the input power requirements of the integrated system. In such a case, a PVT collector can either provide higher electrical output by maintaining lower PV surface temperature or provide higher outlet air temperature resulting in lower electrical output. Although, the latter will greatly help in the operation of SDC system, prolonged operation with such high outlet air temperature will result in higher PV surface temperature as well, in turn, adversely affecting the material integrity of the PV modules.

In order to maintain high PV cell efficiency and material integrity for longer time, PV surface temperature need to be maintained under a certain temperature. This results in use of an auxiliary heater to boost the outlet air temperature to the required level to support the SDC system's operation, thereby increasing the electricity consumption of the integrated system.

Therefore, using a Solar Air Heater (SAH) in series with a PVT collector can help boost the outlet air temperature and reduce the input power requirement of the integrated system.

1.3 Objective

The objective of this research is to develop an integrated design methodology for a photovoltaic thermal solar air heater (PVT-SAH) assisted solid desiccant cooling (SDC) system in hot and humid climates, by investigating the design solutions that reduce the integrated system's reliance

on auxiliary heat source, at the same time optimize the solar energy gains (electrical and thermal) for space cooling application.

1.4 Thesis Outline

Chapter 1 provides a background about the cooling energy consumption in buildings and building-related emissions in hot and humid climates. The problems to be considered in this study and the objectives of this study are also presented in chapter 1.

Chapter 2 reviews the literature which outlines the applications of solar technologies in buildings, and methods investigating the performance improvements in solar-assisted cooling technologies with an emphasis on solar-assisted Solid Desiccant Cooling (SDC) systems. Lastly, the potential areas and scope of this research are presented.

Chapter 3 presents the proposed methodology for this research, including integrating PVT-SAH assisted SDC system with proposed modifications, identifying the design parameters and the formulation of optimization problem, and investigating design solutions through multi-objective optimization.

Chapter 4 presents a case study for application of the integrated system for a retail store in a typical low-rise mixe-use building in hot and humid climate. The energy modeling approach for the development of bulding and the PVT-SAH assisted SDC system is also detailed here. Finally, the design parameters to be considered for the optimization analysis are presented, using the integrated system in the case study as a baseline.

Chapter 5 presents and discusses the results of case study, sensitivity and optimization analysis.

Chapter 6 provides a summary of this work with conclusions, and future work opportunities.

Chapter 2. Literature Review

2.1 Applications of Solar Technologies in Buildings

Annually, the earth receives 1.53×10^{18} kWh (1367 W/m^2) of solar radiation onto the surface of the atmosphere, making the sun the most abundant of all available energy sources (Reinhart, 2014). In contrast, the rate of annual world energy consumption is much lower at 1.54×10^{14} kWh. As such, harnessing the available solar energy through different solar technologies can greatly help sustain today's energy requirements. Solar technologies that convert solar radiation into electricity and heat are expected to hold the largest share of renewable energy production in the future.

In buildings, solar energy can be utilized mainly to produce electricity and thermal energy. Flat plate photovoltaic collectors (PV) are most commonly used for electricity production. The PV technology can be mounted on the roof as raked systems (Building Applied Photovoltaic or BAPV) or integrated with the building roof or façade as part of the building envelope (Building Integrated Photovoltaic or BIPV). Solar thermal collectors are used primarily for heating applications such as solar domestic hot water and ventilation air preheating. Solar thermal collector is a mature and commercially viable technology for converting solar radiation into thermal energy (Guo et al., 2017). Flat plate and evacuated tube solar thermal collectors are commonly used in building applications.

The performance of PV or solar thermal collectors is determined through their electrical and thermal outputs, respectively. The temperature at which a crystalline, silicon-based PV cell/module operates, greatly impacts its electrical performance. According to the well-established correlation given by (Florschuetz, 1979)(Skoplaki & Palyvos, 2009),

$$\eta_{PV} = \eta_{STC}(1 - \beta_{PV}(T_{PV} - T_{STC})) \quad (2.1)$$

Where η_{PV} is the PV electrical efficiency calculated based on the cell temperature (T_{PV}), η_{STC} is the PV electrical efficiency under standard conditions, β_{PV} is the temperature coefficient of the module (typically $-0.5\%/^{\circ}\text{C}$), T_{PV} is the PV module surface temperature and T_{STC} is the PV module surface temperature (25°C) at which reference PV electrical efficiency is given. As per equation 2.1, the electrical efficiency of PV will decrease with the increase in the PV's operating temperature. As such, in locations with hot climates, the electrical performance of solar PV collectors will be hindered.

The total thermal energy extracted from the PVT-SAH is given by,

$$Q_{air} = \dot{m}C_p(T_o - T_{in}) \quad (2.2)$$

Where Q_{air} (W) is the thermal energy extracted by the circulating air, \dot{m} (kg/s) is the mass flow rate of air, C_p (J/kg $^{\circ}\text{C}$) is the specific heat of air, T_o ($^{\circ}\text{C}$) is the temperature of air at the outlet of PVT-SAH, T_i ($^{\circ}\text{C}$) is the temperature of air at the inlet of PVT-SAH. A solar thermal collector's thermal output is dependent on the mass flow rate and the temperature differential between inlet and outlet of the collector.

The individual application of PV and solar thermal technologies poses a few disadvantages.

- Extremely hot ambient conditions degrade the electrical performance of the PV technology.
- Solar thermal collectors require large areas to produce useful thermal energy at required temperatures (for example, solar domestic hot water requires at least 60°C outlet temperature).
- Also, depending on the requirements of a building and the area available for the application of solar technologies, it becomes difficult to use both the technologies mentioned above.

A flat plate Photovoltaic and Thermal (PV/T) collector is the integration of both PV and solar thermal technologies into one combined unit. This type of collector serves two main purposes: it improves the overall electrical output, and the excess heat can be extracted as useful thermal energy. This way, it can overcome the disadvantages of the individual application of flat plate solar PV or solar thermal collectors (Guo et al., 2017). Several studies discussing the performance of BIPV systems and Building Integrated Photovoltaic Thermal (BIPV/T) systems have been conducted; the latter has the better electrical performance and offers additional gains through the thermal energy output (Yang & Athienitis, 2016).

2.2 Solar-assisted Cooling Technologies

The focus of this thesis is on locations with hot and humid climates. ASHRAE Standard defines these types of climates into following categories (ASHRAE Standard 169, 2013),

Zone Number	Zone Name	Thermal Criteria (SI units)
1A	Very hot and humid	5000 < CDD 10°C
2A	Hot and humid	3500 < CDD 10°C < 5000
3A	Warm and humid	2500 < CDD 10°C < 3500

Table 1 Classification of Relevant Climate Zones

Cooling Degree Days (CDD) quantifies the amount (in degrees) and the duration (in days), the outside air temperature was above certain level in a location. The climates characterized by hot and humid ambient conditions need air conditioning systems for space cooling in buildings. Conventional air conditioning systems require high-grade energy in the form of electricity to fulfill the space cooling demand. The building sector is accountable for more than half of the world's total electricity consumption. Of all the different end-uses, space cooling has a major share of building energy consumption. Simultaneously, space cooling technology used in most buildings is also responsible for building-related CO₂ and GHG emissions, either directly or indirectly (IEA, 2018)(Global Alliance for Buildings and Construction, 2016).

Currently, most of the space cooling demand in buildings is fulfilled by VCR systems (Guo et al., 2017). In hot and humid climates, dehumidification in VCR systems is achieved by cooling of highly humid air to the dewpoint temperature. Thus cooling the supply air beyond the required room setpoint (Ahmed et al., 2005), making the system energy intensive and inefficient when handling air with high moisture content (Fan et al., 2019)(Jani et al., 2016). Also, most of the space cooling demand peaks during the daytime hours resulting in additional load on the electrical grid. As a result, VCR systems, even though technologically more advanced than many other existing space cooling technologies, present certain disadvantages in energy efficiency, cost-effectiveness, sustainability, and environmental impacts (Guo et al., 2017). Since cooling loads mostly coincide with the high solar irradiation, solar-assisted cooling technologies have been considered as

alternatives to conventional cooling technologies mainly because of their potential to reduce electrical energy consumption as well as peak demand. Thermally driven cooling technologies use thermal energy for their operation. At the same time, some solar-assisted cooling technologies can also produce electricity, which can offset the electrical energy requirements of solar-assisted cooling systems.

Solar-assisted cooling technologies can be mainly divided into two categories: First, conventional VCR systems powered by the electricity generated using on-site solar PV. Second, thermally activated/driven cooling technologies (mainly absorption, adsorption, and desiccant cooling), which use solar thermal energy for their operation (Eicker, 2014)(Guo et al., 2017).

The continuous cost reductions in PV technology have resulted in the electricity prices reaching almost grid parity in some places (Guo et al., 2017). At the same time, electrical vapor compression systems continue to benefit from improved research and boost a very good coefficient of performance. These reasons make solar PV cooling a very attractive option. However, this integrated system still uses the VCR system for space cooling, which suffers from inefficient operation in extremely hot and humid climates, making it unsuitable.

On the other hand, solar thermal collectors benefit from a better collector efficiency compared with solar PV collectors. However, thermal cooling systems suffer from a low thermal coefficient of performance. This also means that a coupled solar thermal cooling system will need a larger collector area to supply the thermal energy required for the less efficient thermal cooling technology. Also, thermal cooling systems are mostly available in larger sizes making the smaller systems expensive (Guo et al., 2017).

A PVT collector coupled with a thermally driven cooling technology overcomes the aforementioned solar-assisted cooling technologies' main issues. A PVT assisted thermally driven cooling system can offer a more efficient and cost-effective solution since it converts the incoming incident solar radiations into thermal and electrical energy (Guo et al., 2017).

There are four most commonly used thermally driven cooling technologies that exist in the industry – absorption, adsorption, liquid desiccant, and solid desiccant cooling. Absorption and adsorption cooling technology work similarly to conventional VCR technology. In that, a refrigerant (usually water, ammonia, carbon dioxide) is used to provide the cooling effect as it gets evaporated at low temperature and low pressure. The refrigerant needs to be compressed to condense at room temperature or cooling tower temperature. In VCR systems, this is achieved through mechanical compression. However, in absorption or adsorption systems, the refrigerant is either absorbed (solution) or adsorbed (adsorbent bed), heated, and expelled to the condenser, wherein the refrigerant vapors cool down into liquid state. This type of cooling can achieve a chilled water temperature of up to 6°C (Eicker, 2014). Liquid and solid desiccant cooling technologies are usually called open sorption cooling. Desiccant cooling systems supply air as a cooling carrier (Eicker, 2014). Incoming process air (supply air) is passed through a desiccant bed (liquid or solid), where the desiccant material absorbs the moisture in the air, increasing the air temperature. The process air undergoes sensible cooling and humidification through a sensible heat exchanger and a direct or indirect evaporative cooler. It is necessary to desorb the desiccant

material (sorbent), which is achieved by passing hot air over the desiccant bed. Generally, desiccant cooling systems require low temperature for regeneration of the desiccant material (Eicker, 2014)(Guo et al., 2017).

This study aims to integrate an air-based flat plate PVT collector with a thermally driven cooling system for space cooling applications in buildings. Therefore, thermally driven cooling technologies that require a low operating temperature (<80°C) and offer a good coefficient of performance are considered for this study.

Table 2 presents a performance overview of solar thermally driven cooling technologies based on several studies.

Cooling Technology	Regeneration Temperature (°C)	COP	References
Solar thermal absorption	70-110	0.6-0.82	(Florides et al., 2002) (Mateus & Oliveira, 2009) (Henning, 2007) (Eicker, 2014)
Solar thermal adsorption	55-100	0.43-0.77	(Fong et al., 2010)(Henning, 2007) (Eicker, 2014)
Liquid desiccant cooling	65-100	0.6-0.8	(Gommed & Grossman, 2007)(Sahlot & Riffat, 2016)
Solid desiccant cooling	55-90	0.5-1.1	(Fong et al., 2010) (H. Li et al., 2011) (Eicker, 2014)(Sahlot & Riffat, 2016)

Table 2 Performance Overview of Solar Thermally-driven Cooling Technologies

Based on the summary of the performance overview presented in the table above, it is observed that the Solid Desiccant Cooling (SDC) technology offers comparatively better COP at lower regeneration temperatures than the other available solar thermally driven cooling technologies. Therefore, this study focuses on solar-assisted solid desiccant cooling systems.

2.3 Solar-assisted Solid Desiccant Cooling (SDC) systems

This research focuses on a flat plate Photovoltaic and Thermal Solar Air Heater (PVT-SAH) assisted Solid Desiccant Cooling (SDC) system. The performance of a PVT-SAH depends mainly on solar radiation and the PV surface temperature (Al-Waeli et al., 2017). A higher mass flow rate of air through an air channel under the PV modules facilitates the heat transfer, which in turn leads to lower PV surface temperature. Several studies have been conducted to improve the performance of PV/T collectors. These include the addition of a glazed/insulated transparent cover on top of the PV (Tripanagnostopoulos et al., 2002)(Yang & Athienitis, 2014), attaching metal fins in the air channel (Tonui & Tripanagnostopoulos, 2007)(Fan et al., 2018) and using semi-transparent PV modules (Aste et al., 2008). Although an increase in outlet air temperature means a lower electrical efficiency (Guo et al., 2017), it is possible to use a PVT collector with SAH to boost the outlet air temperature without hindering the electrical performance of the PVT collector. Several studies have investigated the use of PVT-SAH together with the help of Unglazed Transpired Collector

(UTC) (Athienitis et al., 2011), heat pipes (Fan et al., 2019) and glazed solar thermal collector (Pantic et al., 2010). It has been observed from previous studies that PVT-SAH can achieve outlet air temperatures of up to 80°C (Mei et al., 2006)(Tonui & Tripanagnostopoulos, 2007)(Eicker et al., 2010) and significantly higher with solar selective coatings (Fan et al., 2019)(Chow, 2010)(Duffie & Beckman, 2013)(El-Sebaai & Al-Snani, 2010). Assuming daytime operation, PVT-SAHs with high outlet air temperatures can be a reliable and consistent source of regeneration air for a Solid Desiccant Cooling system.

Performance Improvement Methods	Temperature Difference (°C)	References
Additional glazed/insulated transparent cover	12-20	(Tripanagnostopoulos et al., 2002)(Yang & Athienitis, 2014)
Attaching metal fins in the air channel	12-51	(Tonui & Tripanagnostopoulos, 2007)(Fan et al., 2018)
Using semi-transparent PV modules	Upto 25	(Aste et al., 2008)
Unglazed Transpired Collector (UTC) in series	6-9	(Athienitis et al., 2011)
Glazed solar thermal collector in series	Upto 45	(Eicker et al., 2010)
Solar selective coatings and heat pipes	Outlet air temperature between 100-200	(Fan et al., 2019)(Chow, 2010)(Duffie & Beckman, 2013)(El-Sebaai & Al-Snani, 2010)

Table 3 PV/T Performance Improvement Methods

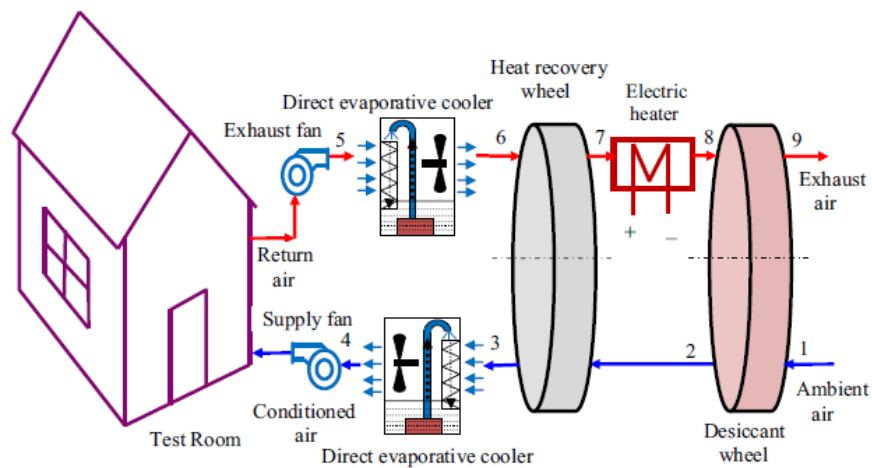


Figure 1 Conventional Solid Desiccant Cooling System in Ventilation Mode (Jani et al., 2016)

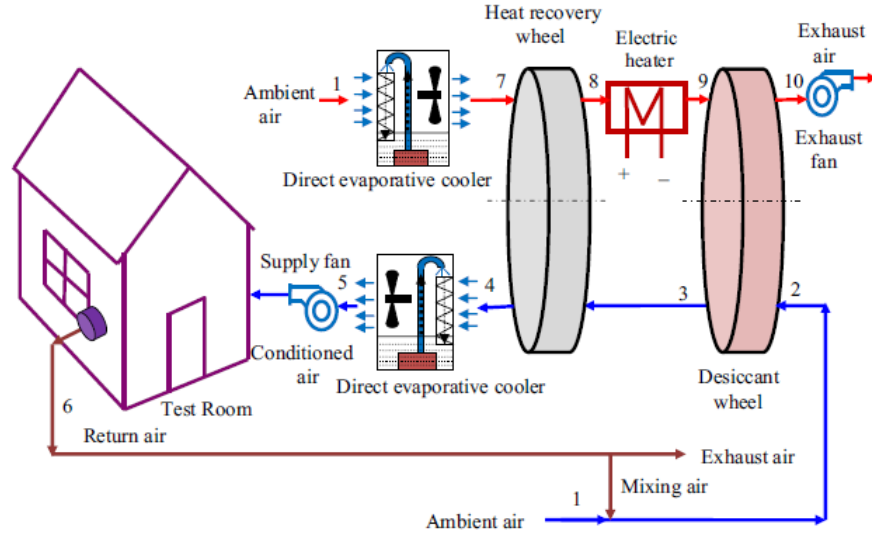


Figure 2 Solid Desiccant Cooling System in Recirculation Mode (Jani et al., 2016)

Figures 1 and 2 illustrate typical Solid Desiccant Cooling (SDC) system configurations in ventilation and recirculation modes. An SDC system mainly consists of three components: desiccant dehumidifier, cooling unit, and regenerative heat source (Daou et al., 2006). The ambient air undergoes dehumidification from 1-2, sensible cooling from 2-3, evaporative cooling from 3-4, and supplied to the space. The desiccant dehumidifier needs to be regenerated to allow continuous dehumidification of supply air. Therefore, a separate stream of ambient air undergoes sensible heating from 7-9 and the heated air is used to desorb the desiccant dehumidifier.

The desiccant material in the desiccant dehumidifier removes moisture from incoming process air (supply air) by adsorbing water molecules on the surface. Thus, it serves the function of handling the latent load. Usually, a slowly rotating dehumidifier wheel packed with desiccant material is employed. The process air leaving the desiccant wheel is drier and warmer than ambient conditions. The ability of the desiccant wheel to remove moisture content from the process air is determined by the desiccant wheel dehumidification efficiency and expressed as,

$$\eta_{deh} = \frac{(w_{amb} - w_{process\ DW\ out})}{(w_{amb} - w_{ideal})} \quad (2.3)$$

Where, η_{deh} is the desiccant wheel dehumidification efficiency, w_{amb} is the ambient air specific humidity (g/kg of dry air), $w_{process\ DW\ out}$ is the process air specific humidity at the desiccant wheel outlet (g/kg of dry air) and w_{ideal} is the ideal specific humidity (g/kg of dry air) taken as zero by assuming that the process air is completely dehumidified at the outlet of desiccant wheel.

The cooling unit, usually an evaporator of conventional VCR system, cooling coil, or evaporative cooler, handles the sensible load. In the case of an evaporative cooler, the incoming dry and heated process air is cooled down using the evaporation of water. The supply air temperature attainable using an evaporative cooler is dependent on the wet-bulb temperature of incoming process air. In short, drier process air can achieve lower supply air temperatures using evaporative coolers. The

effectiveness of a direct evaporative cooler is the ratio of the dry bulb temperature difference between the incoming and outgoing process air in the direct evaporative cooler to the temperature difference between incoming dry bulb and wet bulb temperatures of the process air. Direct evaporative cooler effectiveness is expressed as,

$$\epsilon = \frac{(T_{in,db} - T_{out,db})}{(T_{in,db} - T_{in,wb})} \quad (2.4)$$

Where, ϵ is the direct evaporative cooler saturation efficiency (effectiveness), $T_{in,db}$ is the incoming air dry bulb temperature, $T_{out,db}$ is the outgoing air dry bulb temperature (supply air), $T_{in,wb}$ is the incoming air wet bulb temperature.

During the sorption phase, the desiccant wheel adsorbs moisture and may get saturated if it is not supplied with additional thermal energy for desiccant wheel regeneration. This is achieved by using a regenerative heat source: solar heat, waste heat, or heat available through natural gas. The arrangement of the components of an SDC enable it to remove moisture from the air without the need for an additional cooling stage, which is required in conventional VCR systems. As a result, SDC systems provide better control over humidity.

The performance of an SDC system can be evaluated using thermal Coefficient of Performance (COP_{th}) and expressed as (Jani et al., 2016),

$$COP_{th} = \frac{q_{cool}}{q_{heat}} = \frac{\dot{m}_{supply}(h_{room} - h_{supply})}{\dot{m}_{return}(h_{reg} - h_{HX})} \quad (2.5)$$

Where, COP_{th} is the thermal coefficient of performance of the SDC system, q_{cool} is the cooling energy supplied, q_{heat} is the heating energy required, \dot{m}_{supply} is the supply air mass flowrate, \dot{m}_{return} is the return air mass flowrate, h_{room} is the room air enthalpy, h_{supply} is the supply air enthalpy, h_{reg} is the regeneration air enthalpy, and h_{HX} is the enthalpy of air at the outlet of the heat exchanger.

Pennington first proposed the basic cycle of a Solid Desiccant Cooling (SDC) system consisting of a rotary desiccant dehumidifier, a heater, and an evaporative cooler in 1955 (Pennington, 1955). The Pennington cycle used 100% fresh air as supply air and was also called the ventilation cycle. Since then, many studies have been conducted by introducing additional components and creating new configurations to improve this system's performance. For instance, additional heat exchangers were used by Dunkle (Dunkle, 1965). A recirculation cycle helps increase system capacity in a warm and humid climate, by reusing return air at the inlet of the desiccant wheel (Daou et al., 2006). Thorough reviews of various SDC system configurations, including the ventilation cycle, recirculation cycle, Dunkle cycle, SENS cycle, and DINC cycle, have been conducted (Daou et al., 2006)(Jani et al., 2016)(La et al., 2010). They concluded that SENS cycle achieves the best thermal coefficient of performance, although the complexity of this cycle hinders its application. DINC cycle, on the other hand, offers a decent thermal COP of 1.6 at the same time, benefits from a much simpler arrangement of components.

Usually, a desiccant wheel can be regenerated by hot air in the temperature range of 50°C-80°C (Ge et al., 2014)(Gommed & Grossman, 2007)(H. Li et al., 2011)(Jani et al., 2016). Still, it may

require higher temperatures in extremely hot and humid conditions. Therefore, the thermal energy available from a PV/T collector can be enough to regenerate a desiccant wheel. Several studies have been conducted related to the design, feasibility, performance, and optimization of a solar-assisted desiccant cooling systems, especially in a warm and humid climate.

Aste et al. developed and implemented a BIPV/T component design concept that used semi-transparent PV modules for the Fiat Research Centre at Orbassano in Italy. It was observed that this setup could deliver power at 20 kWp, at the same time, the hot outlet air can be used for preheating the ventilation air in winter and for desiccant cooling in summer (Aste et al., 2008).

Shahsavari & Khanmohammadi investigated through a numerical study and multi-objective optimization the energy and exergy performance of an exhaust air heat recovery system consisting of a BIPV/T collector and a thermal wheel (TW). This BIPV/T-TW setup was used to seasonally preheating/precooling the ambient fresh air while producing electricity. Through comparing energy and exergy performance among BIPV/T, TW, and BIPV/T-TW, the authors observed that BIPV/T-TW has the best energy performance among the three systems, whereas, BIPV/T system has better exergy performance. The optimized version of BIPV/T-TW was able to achieve significant improvements in energy and exergy performance (Shahsavari & Khanmohammadi, 2019).

Fong et al. conducted a simulation-based optimization study of a SAH assisted a desiccant cooling system for Hong Kong. They concluded that with such a system, a yearly average solar fraction of 17% and mean COP_{th} of 1.38 can be achieved (Fong et al., 2010).

In another research, Eicker et al. analyzed components performance and seasonal operational experiences of PVT and SAH assisted solid desiccant cooling systems for three different warm and humid locations in Germany, China, and Spain. It was observed that the German installation achieved an average seasonal COP of 1.0, whereas this value was less for the Chinese installation. Another observation from this study was that to achieve higher cooling performance; the system must have lower regeneration temperature and lower dehumidification rates (Eicker et al., 2010).

Li et al. investigated the performance of a SAH assisted desiccant cooling/heating system working in two configurations in China. This system achieved COP_{th} of 0.97 during the cooling season and 0.45 during the heating season (H. Li et al., 2012).

Fan et al. 2019 examined performance evaluation and optimization of a double pass PVT-SAH of varying sizes coupled with a desiccant cooling system. The PVT-SAH incorporated heat pipes to increase the outlet air temperature for desiccant regeneration significantly. The optimized system achieved annual SF and electrical COP up to 96.9% and 19.8, respectively for a commercial building case study in a hot and humid climate. It was concluded that a minimum of 0.35 m² PVT-SAH per m² of the conditioned floor area is required for this type of design of a hybrid cooling system to achieve/exceed a typical COP for commercial buildings (2.6-3.0) (Fan et al., 2019).

When considering operating costs and savings related to them, it is necessary to note that costs depend on the local electricity fares which tend to vary from place to place (Daou et al., 2006).

Mazzei et al. studied the summer operating costs of desiccant and conventional cooling systems for a retail store through software codes. It was observed that desiccant system operating cost savings of up to 35% and thermal cooling power reduction of up to 52% could be obtained (Mazzei et al., 2002).

Although, several studies point out the feasibility and combined potential of PVT-SAH as the only source of regeneration heat, in hot and humid climates, desiccant wheel requires air at even higher regeneration temperature. This results in the use of an auxiliary source of heating to achieve the required regeneration temperature. Therefore, in order to use PVT-SAH as the main source of regeneration heat, it is necessary to look at ways to improve the design of the PVT-SAH assisted solid desiccant cooling system and minimize the use of auxiliary heater. Increase in the outlet air temperature of the PVT-SAH directly impacts the electrical performance of the PVT collector. This poses an optimization issue as both electricity production and higher outlet air temperature are desirable in case of an integrated PVT-SAH assisted SDC system.

2.4 Optimization of Solar-assisted SDC systems

The performance of an integrated PVT-SAH assisted SDC system can be affected by many parameters. This has been investigated through some studies. (Eicker et al., 2010)(Mei et al., 2006) obtained regeneration air between 50-70°C for solar air collector area of 100 m², channel heights between 0.095-0.14 m, regeneration mass flowrate up to 3.05 m³/s and average air velocity less than 9 m/s. They concluded that the regeneration air temperature at 70°C and above was enough to regenerate the desiccant wheel while keeping the regeneration air flowrate between 0.833-2.5 m³/s and average velocity between 3-9 m/s (Mei et al., 2006).

An optimization study was conducted by (Farshchimonfared et al., 2015) to optimize the channel height, air mass flow rate and air distribution duct diameter of solar air PVT collectors connected to residential building . It was concluded that optimum channel height value varies between 0.095-0.26 m and this value increases with increase in L/W ratio as well as the collector area.

It should be noted that in many of the previous studies, channel height is around 0.095 m. The main reasons for this are higher volumetric mass flow rate, higher average flow velocity and length of the solar air collectors (Aste et al., 2008)(Eicker et al., 2010). (Chung & Lee, 2011) conducted a simulation study and concluded that amongst several design parameters, impact of regeneration temperature is most dominant on the COP of a solid desiccant cooling system. These studies individually point out the significance of many different design parameters of PVT collectors and solid desiccant cooling systems.

(Tiwari & Sodha, 2007) pointed out that only parametric analyses have been performed in several studies aiming to improve the performance of PVT collectors coupled with air conditioning systems. These types of parametric studies lack comprehensive investigation of all possible designs. It has been observed in some previous studies that both the electrical and thermal energy production of PVT-SAH were aggregated and considered as a single indicator (Sobhnamayan et al., 2014). However, as mentioned in the previous section, based on varying designs of PVT collector, the electrical and thermal energy production can have conflicting relationship with each other. Therefore, it is important to perform a multi-objective optimization study in order to

optimize the PVT-SAH assisted solid desiccant cooling system by considering wide range of important parameters and different configurations.

There are few studies involving multi-objective optimization for water-based and air-based BIPV/T collectors (Fan et al., 2019). Among the air-based solar collector studies, some performed optimization only for heating purposes by transferring the outlet air of the BIPV/T directly through the air handling unit.

(Z. X. Li et al., 2019) conducted an optimization study in which ambient air passing through an earth air heat exchanger entered a BIPV/T collector which was used for preheating the building. The objective of this study was to maximize the total annual energy and exergy outputs of the BIPV/T collector.

In another study, (He et al., 2020) conducted an optimization study to maximize the annual average exergo-economic performance of a coupled BIPV/T and sensible rotary heat exchanger system by optimizing the geometric and operating parameters of the system. It was reported that through a multi-objective genetic algorithm (MOGA) optimization, the annual average enviro-economic and exergo-economic aspects of the optimized system were 36.8% and 23.1% higher than the baseline system, respectively.

A multi-objective design optimization methodology for a PVT-SAH system was developed by (Fan et al., 2018). First, a sensitivity analysis was performed to reduce the number of parameters followed by an optimization study. The objective of the study was to increase useful thermal energy (thermal energy with air temperature greater than 60°C) and net electricity gains (PV electricity production minus fan power) considering the most influencing parameters. It was reported that the optimization resulted in increase in the thermal energy and net electricity gains by 21.9% and 20% respectively in comparison to the baseline design.

Most of the previous studies have considered optimization of either the PVT collector, PVT-SAH or other cooling systems separately. However, this does not take into account the interaction between all the components of the integrated system and leaves a gap in optimization. When considering application of an integrated PVT-SAH assisted SDC system, it would be much better to consider optimizing the design parameters of the entire integrated system. In this regard, for instance, no previous work has been conducted to maximize PV electrical energy gain and minimize solid desiccant cooling system's (auxiliary heater) energy consumption as they have a conflicting relationship with each other.

2.5 Potential Areas and Scope of this Research

Integrated PVT-SAH assisted SDC systems (PVT-SAH SDC) combine to form a very interesting approach towards resolving multiple shortcomings of either systems when used individually. Firstly, PVT technology serves to improve the electrical output of conventional PV collectors by introduction of air channel under the PV modules to remove the excess heat. Secondly, SAH technology serves to boost the temperature of air coming from the PVT collector even further, making it suitable for use as regeneration heat source for an SDC system. And finally, using an SDC system as a substitute or even in conjunction with a conventional VCR system can solve

issues associated with the latter's energy intensiveness and inefficiency in hot and humid climates. An Integrated PVT-SAH assisted SDC system potentially offers a great alternative to conventional space cooling approach at the same time being able to produce surplus electricity and reduce the dependence on the electrical grid, thereby, reducing associated indirect CO₂ and GHG emissions.

In case of the integrated PVT-SAH assisted SDC systems, there are many areas that show potential for research investigation whether individually or as a combined system. These can be mainly divided into two categories: Reduction in desiccant regeneration temperature and increase in the PVT outlet air temperature. (Guo et al., 2017) concluded that desiccant regeneration temperature can be reduced to below 60°C by pre-cooling of entering process air, performing post-dehumidification sensible cooling without moisture addition, using internally cooled dehumidification and two-stage dehumidification. Several studies have been conducted to increase the outlet air temperature of PVT. From these studies it was observed that addition of glazed cover, integrating two types (PVT and SAH) solar air collectors, proper air channel design (channel height, L/W ratio, flowrate etc.), and addition of fins inside the air channel are few ways to improve the overall performance of the PVT-SAH.

There are many aspects of an integrated PVT-SAH assisted SDC system that can be improved and optimized. However, applying all the performance improvement methods mentioned above will require more components, leading to a more complex integrated system configuration. Also, leaving out certain improvements methods, does not significantly impact the outcome of this study. **This study aims to optimize the overall performance of an integrated system configuration without increasing the system complexity. Therefore, this study mainly focuses on an integrated air-based roof Photovoltaic Thermal Solar Air Heater (PVT-SAH) assisted single-stage Solid Desiccant Cooling (SDC) system for a hot and humid climate.**

Chapter 3 Methodology

In this thesis, an integrated design methodology for a Photovoltaic Thermal Solar Air Heater (PVT-SAH) assisted Solid Desiccant Cooling (SDC) system in hot and humid climates is proposed. The first step involves identification and selection of a solar technology for utilizing locally available solar energy resources to the fullest potential, and a suitable thermally driven cooling technology that helps to maintain thermal comfort. The second step involves integrating the selected systems into an appropriate configuration that offers the best results for the design conditions. The third and final step involves investigation of different design solutions for application of the integrated system in hot and humid climates. Simultaneous simulation-based investigation of different designs is conducted employing energy modeling and optimization.

The design methodology is incorporated in a case study for application of a solar-assisted SDC system for air-conditioning of a retail store of a typical multi-story low-rise mixed-use building complex located in a hot and humid climate. Three different integrated system configurations are compared to identify which configuration performs the best out of the three and this configuration is optimized further to improve the the integrated system's overall performance. The results of the case study are used to showcase the potential of the proposed design methodology.

3.1 Integrated PVT-SAH assisted SDC system configuration

Solar-assisted Solid Desiccant Cooling systems (SDC) have been garnering attention as an alternative to conventional cooling technologies for a long time (Jani et al., 2016). Several studies have investigated solar-assisted SDC system's configurations, application potential, and feasibility in different climatic conditions. However, many of the previous studies use typical configurations with either ventilation or recirculation modes of operation. For instance, in a typical solar-assisted SDC system configuration, the air coming out of the sensible heat exchanger is exhausted to the surroundings (open exhaust air discharge approach). Also, ambient air is used at the inlet of the solar collector on the regeneration side. However, using part of recirculated air on the regeneration side offers favorable results in hot and humid climates, mainly better supply air conditions if sufficient fresh air supply is maintained to avoid any associated indoor air quality problems. This section discusses the identification, selection, and integration approach for a solar-assisted SDC system in recirculation mode and proposes modifications to an existing configuration to obtain the best results in hot and humid climates.

3.1.1 Identification and selection of solar and thermally driven cooling technologies

Among the liquid-based (water) and air-based solar PVT technologies, the water-based technologies certainly have a significant advantage over the air-based technologies in terms of heat transfer and thermal storage capacity. In contrast, the air-based technologies benefit from no leakage, lower weight of the entire assembly, lower initial costs, and lower maintenance costs and effort (Yang & Athienitis, 2016). In building rooftop application, flat-plate PVT collectors can be easily mounted or integrated, making them a good choice from both engineering and architectural perspectives. Closed-loop air-based flat-plate PVT collectors can supply low-grade thermal energy, however connecting a flat-plate solar thermal collector to the outlet of the PVT collector

helps to boost the outlet air temperature even further. The combination of flat-plate PVT and solar thermal collectors can result in outlet air temperatures of up to 80°C (Mei et al., 2006)(Eicker et al., 2010)(Tonui & Tripanagnostopoulos, 2007). Based on this, a Photovoltaic Thermal Solar Air Heater (PVT-SAH) system is proposed to utilize the solar energy gains (electrical and thermal) to the fullest potential and to supply the required heated air to the thermally driven cooling system.

Through the literature review, based on different performance characteristics and scope of this research, a Solid Desiccant Cooling (SDC) system is identified as the cooling technology. Also, an SDC system synergizes quite well with a PVT-SAH since both are air-based systems and the available heated air from the PVT-SAH can be easily supplied to the SDC system without the need of additional heat exchanger (air-to-water heat exchanger). Simultaneously, the range of outlet air temperature attainable through a PVT-SAH system complements the range of regeneration air temperature requirements of an SDC system.

3.1.2 Integration of the PVT-SAH and SDC system into an appropriate configuration

The arrangement and connections of each component of the integrated system along with the mode of operation greatly impact the system's overall performance.

Previously several studies have been conducted to investigate and introduce different configurations. The Direct Indirect Evaporative Cooling (DINC) cycle offers a very good balance of performance and simplicity (Jani et al., 2016). In recirculation mode, return air from the conditioned space is reused at the desiccant dehumidifier's inlet, which increases the system capacity in warm and humid climates (Daou et al., 2006). It should be noted that an SDC system achieves cooling and dehumidification mainly through ventilation and air circulation. Also, high fresh airflow rate is necessary for such systems due to the indoor air quality problems associated with the use of evaporative coolers. Therefore, traditionally, these systems have operated in ventilation mode (100% fresh air supply). However, a significant reduction in fresh air requirement can be achieved when the integrated PVT-SAH assisted SDC system operates in recirculation mode. Based on this, an SDC system using DINC cycle and working in recirculation mode selected for this research.

One critical aspect of this research is the interaction between the PVT-SAH and the SDC system. These interact with each other on the regeneration side. Figures 3, 4 and 5 show three configurations selected for this research – first two represent typically used configurations, while the third represents an existing configuration with some modifications. In the third configuration, a warm mixture of return air and ambient air exiting the sensible heat exchanger (Sensible Wheel or SW) enters the PVT-SAH, which heats the air further, and is used for regeneration of the desiccant dehumidifier (Desiccant Wheel or, DW). The air mass flow rate plays an important role on both supply and regeneration sides. The comparison of performance between these configurations is explained further in chapter 5.

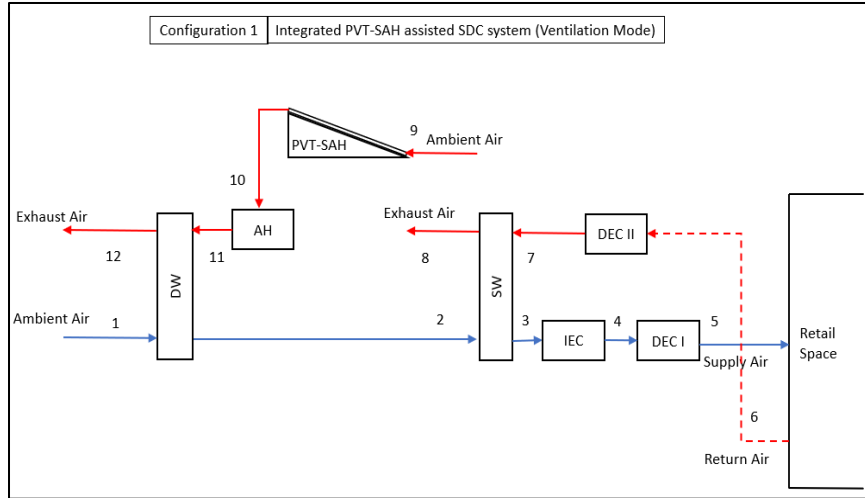


Figure 3 Typical integrated PVT-SAH assisted SDC system configuration 1 (Ventilation Mode)

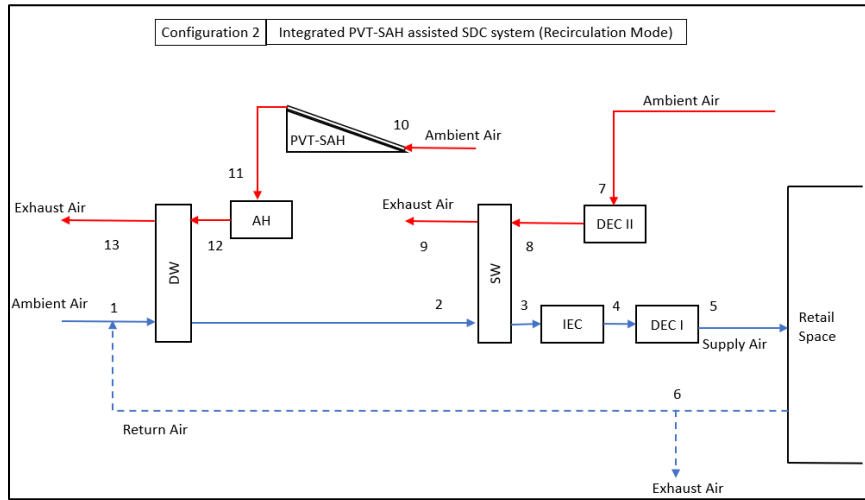


Figure 4 Typical integrated PVT-SAH assisted SDC system configuration 2 (Recirculation Mode)

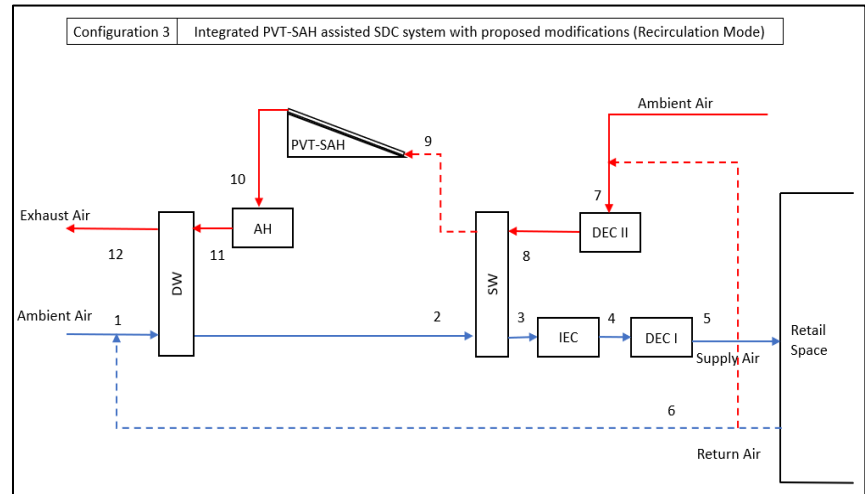


Figure 5 Integrated PVT-SAH assisted SDC system configuration 3 with proposed modifications (Recirculation Mode)

3.2 Identification of Design Parameters and Formulation of Optimization Problem

Many design parameters can be considered in the case of an integrated PVT-SAH assisted SDC system. For instance, air mass flowrate is an important design parameters for both the PVT-SAH and the SDC systems. However, all the design parameters associated with the integrated system do not directly affect the overall performance. In this research, the third configuration discussed in the previous section is used for the optimization analysis.

The overall performance of the integrated system can be evaluated through different performance indicators. Some performance indicators, such as the pressure drop, and the fan consumption, have been considered in the case study's developing of PVT-SAH model section. Whereas, some other component-level performance indicators have been assumed from literature. Considering the interaction of PVT-SAH with the SDC system, this study emphasizes on improving the electrical and thermal performance of the PVT-SAH assisted SDC system and reducing the system's reliance on an auxiliary heater. Therefore, PV electrical energy gain and Auxiliary Heater (AH) energy consumption are employed as two objective functions, to facilitate the sensitivity analysis and formulate the design optimization strategy.

The purpose of sensitivity analysis is to develop a good understanding of the relationship between the design parameters and the objective functions (Fan et al., 2018). Sensitivity analysis is useful to exclude certain design parameters from the optimization problem and to reduce the overall computational time. Commonly used methods for sensitivity analysis include but not limited to One at a Time (OAT), regression analysis, and variance-based methods. The OAT approach does not allow full exploration of input variables, as it considers one varying input at a time while other variables are kept constant. The regression analysis is suitable when the relationship between input and output variables is linear. The variance-based method allows a complete exploration of input variables, accounts for the interaction between the input and output variables, and is suitable for non-linear model responses. In this study, sensitivity analysis is performed with the help of ANOVA (Analysis of Variance). ANOVA is a collection of statistical models used for analyzing the differences in the means of sample groups and the associated variation among the group members and between the sample groups. ANOVA is useful for testing the means of three or more groups. In this research, five design parameters related to the solar-assisted SDC system have been considered for the sensitivity analysis. The design parameters considered are collector area (m^2), collector L/W (length-by-width ratio), PV covering factor (determines the ratio of PVT to SAH), air channel height (m), and air mass flow rate (kg/s). The details of sensitivity analysis are explained in Chapter 4.

3.3 Multi-Objective Optimization to Investigate the Design Solutions

The PV modules' operating temperature constrains the PVT-SAH's ability to produce electricity and heated air outlet temperature, making it difficult to optimize the two objective functions without considering the effect of high PV surface temperature. Therefore, the PV surface temperature is taken as a constraint to ensure good electrical and thermal performance without sacrificing the PV modules' material integrity.

Multi-objective Genetic Algorithm (GA) optimization technique is used to accommodate the multi-criteria decision-making procedure for optimizing the integrated PVT-SAH assisted SDC system. GA helps to retain excellent non-dominated solutions with the help of an efficient multi-search elitism (Poles, 2003). Through GA, it is possible to search a diverse set of solutions with more variables that can be simultaneously optimized (Zolpakar et al., 2020) without prematurely converging to a local optimum. One of the main benefits of GA is the improvement in convergence of the algorithm, ensuring a greater fitness of each new generation in comparison with the fitness of the parent generation. Solutions of GA are represented using the Pareto fronts. A Pareto front is a set of non-dominated solutions frontier (Pareto optimal set), being chosen as optimal if no objective function can be improved without sacrificing at least one other objective (Reddy & Kumar, 2015). The Pareto based multi-objective optimization is advantageous because it provides insight into the trade-off relationships between the objective functions and helps the decision-making process, which helps to overcome the shortcomings of traditional aggregative methods in which all objectives are combined into a weighted-sum, resulting in only one optimal solution (Fan et al., 2018). Further details of optimization are explained in Chapter 4.

Chapter 4 Case Study

Home to some of the world's largest mega cities, India is a highly developing and one of the highest energy consuming countries after China, the United States and Russia. India's domestic electric energy consumption has been on the rise since 2000 and constituted to 22% (186 TWh) in 2013 (Central Electricity Authority, 2013). With the rising population and residential building development in both rural and urban areas, the country's energy requirements continue to skyrocket. As the residential sector's electricity consumption is predicted to rise by more than eight times by 2050, it is of utmost importance for a country like India to invest its resources in mitigating the escalating energy demand from the residential sector (Shukla et al., 2015).

India benefits from an abundant solar energy resource, making India a great location for application of solar technologies. Indian government has recently initiated policies to encourage the use of PV and BIPV systems to boost the local energy production. India has a decent share of solar domestic hot water and PV installations. However, due to the high population density and low space availability for solar parks, it is difficult to find land for new installations. At the same time, largely accessible unused roof spaces are attracting people's attention towards rooftop PV application (Shukla et al., 2015). An energy generation target of 100 GW through solar energy by 2022, has made solar energy one of the fastest growing clean technologies in India. At the same time, solar energy has become cheaper than commercial and industrial power in India (The World Bank, 2017). However, recent trend shows that although commercial rooftop PV installations have increased, residential rooftop PV installations are lagging owing to the local net metering programs and large upfront investment costs associated with PV (UN, 2017).

The IC-IMPACTS project "Solar Energy Powered Net-Zero Energy Smart Buildings" focuses on a typical multi-story low-rise mixed-use (residential/light commercial) building complex. The project aims to achieve the goal of NZEB for common building typologies considering the local climate and construction practices. Simultaneously, ensuring yearly energy produced from locally available renewable resources is equal or more than the energy consumed by the building.

4.1 Location Analysis

India is characterised by having a predominantly hot climate with the climate getting milder as we go from the south to north of the country. Many of the big cities in the country come under hot and humid climate. It is therefore imperative that a location representing such a climate must be chosen. Chennai is a coastal city located in the south Indian state of Tamil Nadu and is classified under hot and humid climate (ASHRAE Standard 169, 2013) Figures 6 and 7 illustrate the annual Global Horizontal Irradiance(GHI) and average air temperature characteristics of Chennai, India. Figures 8 and 9 illustrate the monthly profiles for average air temperature, relative humidity, GHI and cloud coverage. During summers daytime air temperatures in Chennai can go up to 45°C with high relative humidity. At the same time, typical high GHI during summers, makes Chennai a suitable location to investigate the application of solar-assisted SDC system.

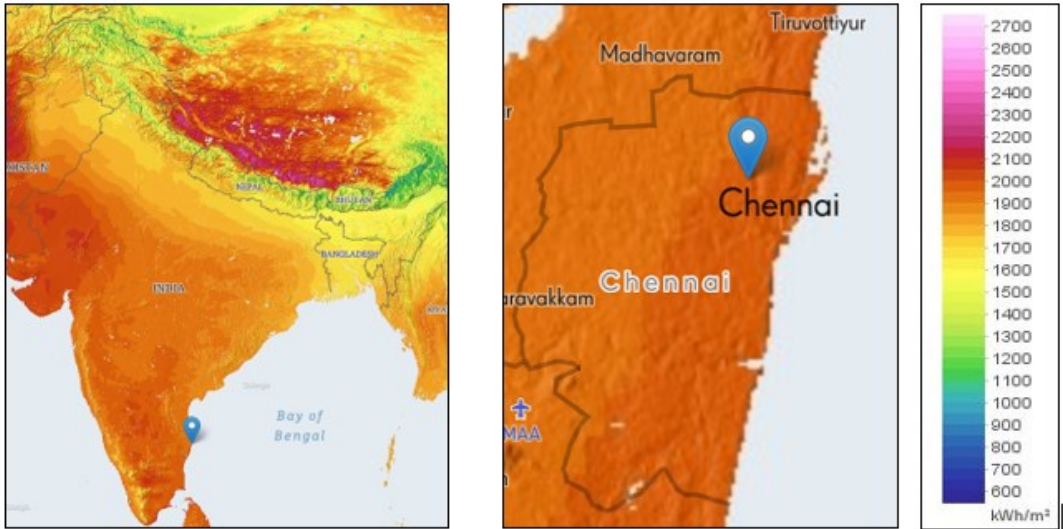


Figure 6 Annual Global Horizontal Irradiance (GHI) in Chennai, India (Kruglov et al., 2018)

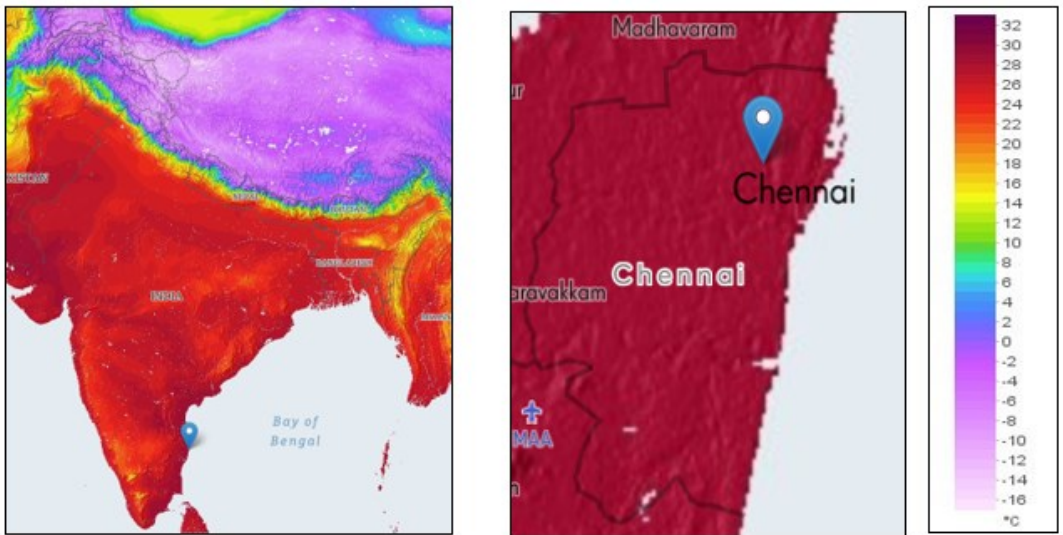


Figure 7 Annual Average Air Temperature in Chennai, India (Kruglov et al., 2018)

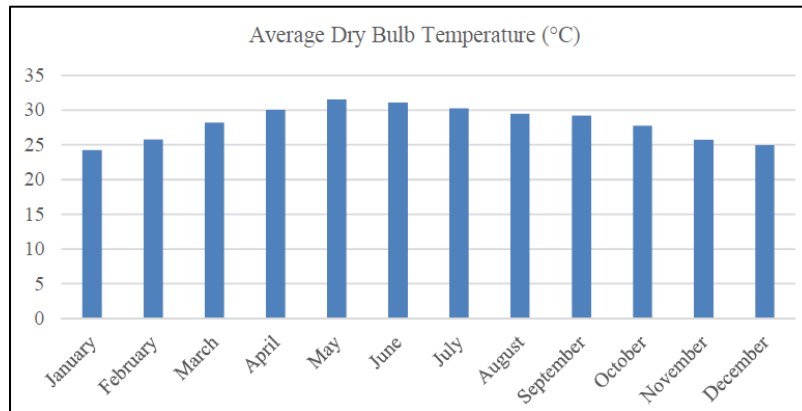


Figure 8 Monthly Profile of Average Dry Bulb Temperature in Chennai (Kruglov et al., 2018)

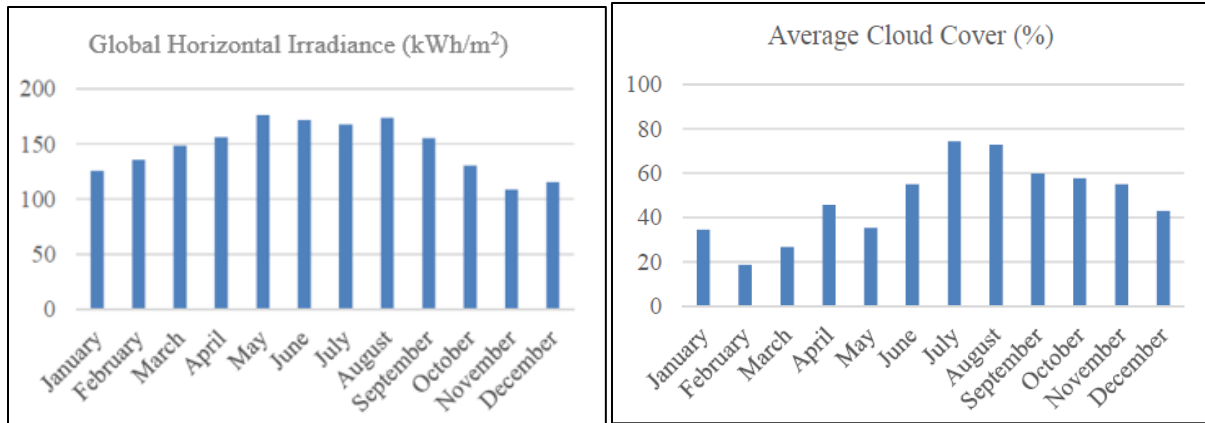


Figure 9 Monthly Profiles of Global Horizontal and Average Cloud Cover Irradiance in Chennai (Kruglov et al., 2018)

4.2 Developing of the Building Energy Model

This section details the process of 3D modelling of a typical building followed by energy simulations to determine the corresponding building energy performance. The building energy model considers external factors such as weather and other physical characteristics and internal factors such as building envelope characteristics, equipment, lighting and occupancy loads, etc. responsible for building energy demand. Understanding a building's energy demand is critical in sizing the capacities of the heating, ventilation and air conditioning (HVAC) systems to be used. At first, considering ideal air loads, the energy demand of the building is determined. Then, the baseline model of the integrated PVT-SAH assisted SDC system connected to the building energy model is simulated to investigate the energy performance of the integrated system.

4.2.1 Building Description

Common building typologies representing multi-story low-rise mixed-use buildings from India were selected to identify and model a typical building. Figure 10 illustrates typical buildings with their construction details from Chennai and the state of Tamil Nadu in India.

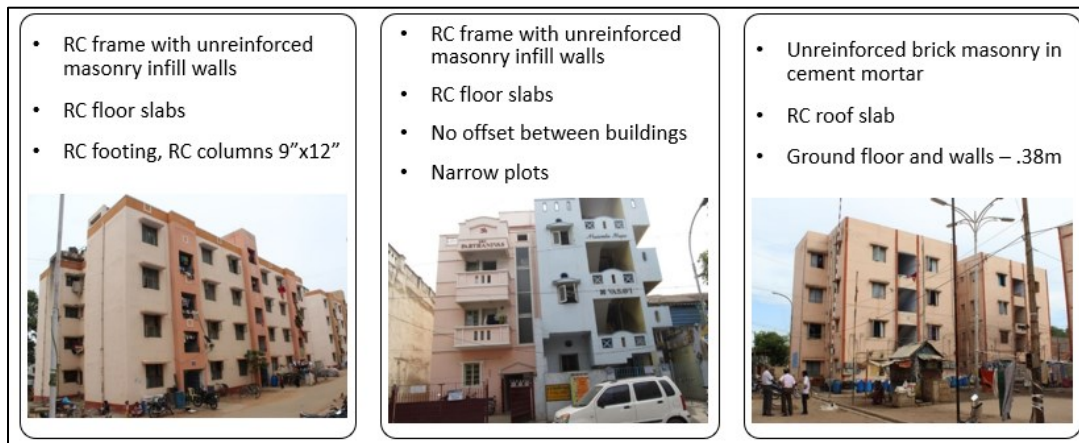


Figure 10 Common Building Typologies in the state of Tamil Nadu, India (National Disaster Management Authority, 2013)

Based on the available information, 3D model of a south-facing 4-story mixed-use building was developed using TRNSYS 3D plugin in SketchUp. The ground floor consists of two retail stores 50 m² each and parking behind the stores. The three floors on top consist of two 45 m² and two 55 m² residential units per floor. The building is not fully conditioned as is the case in India. Only the retail spaces are conditioned; in contrast, the residential apartments have been divided into conditioned and unconditioned zones. Figure 11 illustrates the 3D building model, highlighting one of the retail stores.

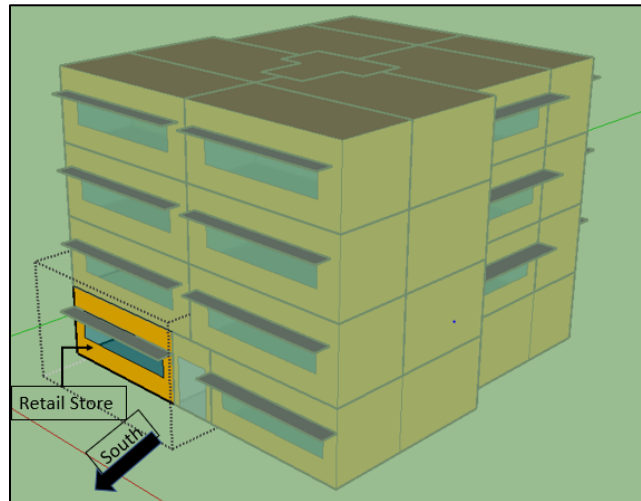


Figure 11 3D Rendering of the Building Model

The building envelope properties follow the requirements stated in the National Building Code of India and Energy Conservation Building Code for Residential Buildings (Bureau of Indian Standards (BIS), 2016)(Bureau of Energy Efficiency (BEE) India, 2018). Table 4 illustrates the building envelope properties. The 3D building model is later imported in TRNSYS 18 and simulated to investigate the building energy performance.

Envelope properties	Case study Building
Wall U-value (W/m ² .K)	1.5
Roof U-value (W/m ² .K)	1.0
Window U-value (W/m ² .K)	5.7
SHGC	0.8
VLT	0.85

Table 4 Building Envelope Properties

4.2.2 Weather Data

The weather data used in this case study is a Typical Meteorological Year (TMY) dataset for Chennai, India. Figures 12 and 13 illustrate hourly profiles of key weather data for winter (January 1st) and summer (June 1st) day in Chennai as per the TMY file.

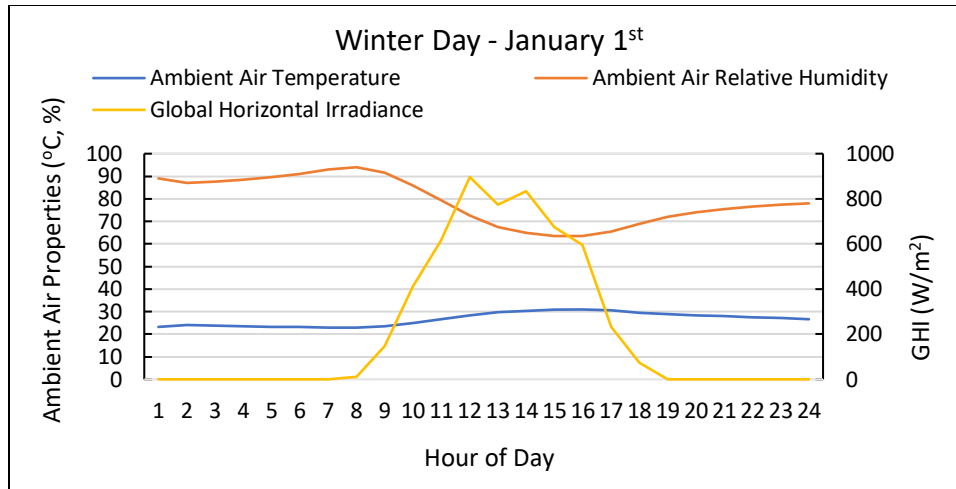


Figure 12 Hourly Profile of Key Weather Data: Winter Day

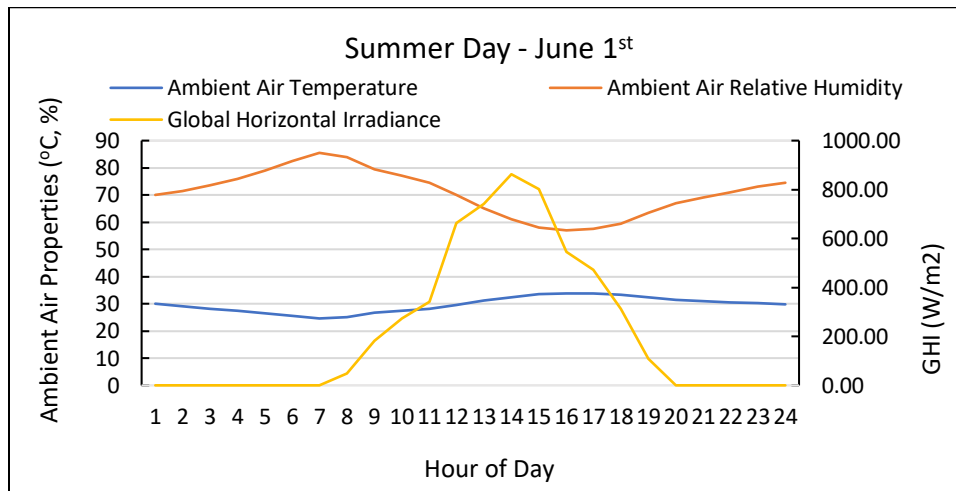


Figure 13 Hourly Profile of Key Weather Data: Summer Day

4.2.3 Lighting, Electric Equipment, Occupancy

The internal gains and schedules for the retail stores and residential units for the 3D model of mixed-use (residential/light commercial) partially air-conditioned building have been assigned as per the ‘Design Guidelines for Energy Efficient Multi-story Residential Buildings’ and ‘US DoE Commercial Reference Building Model of Common Building Stock’ (Bureau of Energy Efficiency (BEE) India, 2016)(Deru et al., 2011). Table 5 illustrates the internal gains through lighting, electric equipment and occupancy for the building.

Internal Gain	Residential		Retail
	Conditioned Space	Unconditioned Space	
Lighting (W/m ²)	4	4	15
Plug Load (W/m ²)	5	7	3
Occupancy (W)	4 x 130	4 x 130	8 x 130

Table 5 Building Internal Gains

4.2.4 Idealized Air Loads

One of the preliminary steps to achieve thermal comfort in buildings requires estimation of the HVAC systems' capacities. According to several norms discussing thermal comfort in buildings, air-conditioning systems for buildings intended for human occupancy should not be sized for more than 26°C for cooling and less than 18°C for heating when occupied (ASHRAE Standard 55, 2013)(Bureau of Indian Standards (BIS), 2016). Also, for locations with high summer temperatures and briefly occurring thermal loads, the maximum allowable rise in the perceived temperature should not exceed 27°C (Eicker, 2014). At the same time, the upper limit for humidity content is 11.5 g/kg or maximum of 65% relative humidity (Eicker, 2014).

An ideal load air system changes the supply air flow rate as per the heating and cooling loads of the building. As per the previously discussed building input characteristics, a hypothetical unlimited cooling capacity HVAC system is used to maintain the desired setpoint zone temperature and relative humidity (below 26°C DBT and 65% RH). The air infiltration is taken as 0.7 air changes per hour to represent a typical Indian building (Bureau of Energy Efficiency (BEE) India, 2016). The simulation is run using all the input design conditions discussed till here for one year using the TMY weather data for Chennai, India.

This thesis aims to reduce the reliance of the integrated PVT-SAH assisted SDC system on auxiliary heat source, at the same time optimize the locally available solar energy. Therefore, the operation of such a system is most suitable during the daytime. The retail store of the building requires cooling during the daytime (9:00 AM-5:00 PM), also this demand coincides with the peak solar irradiation. Based on the previously mentioned points, it is decided that the integrated PVT-SAH assisted SDC system will be sized as per the cooling requirements of the retail store. The peak cooling load for the retail store was found to be 5.42 kW with a sensible to latent heat ratio of 0.60 on May 21st. The cumulative 4h peak cooling load also occurred the same day and was found to be 18.58 kWh.

Surveyed data comprising several similar buildings as the building considered in this study was available through literature. The results of building energy performance simulation have been compared with the available surveyed data for similar buildings.

4.3 Developing of the PVT-SAH assisted SDC System Model

The solar collector considered in this research is a series combination of Photovoltaic Thermal (PVT) collector and Solar Air Heater (SAH). As discussed earlier in chapter 2, the electrical and thermal outputs of a PVT-SAH collector determine the collector's performance. Generally, for a given roof length, solar irradiance, free stream wind velocity, ambient temperature, and air velocity inside the channel are the main parameters that affect the temperatures of PV modules and outlet air [Chen et al. 2010]. Passive cooling of PV (through natural ventilation) is usually inefficient since it only occurs through buoyancy or wind. In contrast, active cooling of PV (through a fan) must consider net electrical efficiency taking into account fan energy use. This fan consumption is typically not more than 5% of the energy recovered from the collector [Athienitis et al. 2010].

In the case of the PVT-SAH, the PVT section of the collector produces electrical and thermal energy, while the SAH section only produces thermal energy. To model the impact of temperature on PV efficiency, the Evans-Florschuetz correlation is used and defined as (Florschuetz, 1979):

$$\eta_{PV} = \eta_{STC}(1 - \beta_{PV}(T_{PV} - T_{STC})) \quad (4.1)$$

Where η_{PV} is the PV electrical efficiency calculated based on the cell temperature (T_{PV}), η_{STC} is the PV electrical efficiency under standard conditions, β_{PV} is the temperature coefficient of the module (typically $-0.5\%/^{\circ}\text{C}$), T_{PV} is the PV module surface temperature and T_{STC} is the PV module surface temperature (25°C) at which reference PV electrical efficiency is given. The PV electrical production depends linearly on the PV modules' operating temperature. Therefore, it is critical to constrain the PV modules' operating temperature to ensure a reasonably high electrical efficiency of the PVT collector. PV temperatures over 70°C cause module deterioration (Yang & Athienitis, 2016) and adversely affect the PV electrical production.

The total thermal energy extracted from the PVT-SAH is given by,

$$Q_{air} = \dot{m}C_p(T_o - T_{in}) \quad (4.2)$$

Where Q_{air} (W) is the thermal energy extracted by the circulating air, \dot{m} (kg/s) is the mass flow rate of air, C_p (J/kg $^{\circ}\text{C}$) is the specific heat of air, T_o ($^{\circ}\text{C}$) is the temperature of air at the outlet of PVT-SAH, T_i ($^{\circ}\text{C}$) is the temperature of air at the inlet of PVT-SAH. Several previously studied thermal performance improvement methods have been discussed in the literature review. A good overall (electrical and thermal) performance of the PVT-SAH without prolonged exposure of PV modules to high temperatures should be of the utmost importance when designing an integrated solar collector system like PVT-SAH.

The wind is responsible for convective losses from the external surface of the PVT-SAH exposed to the surroundings. The PVT-SAH is insulated at the bottom surface to minimize the losses due to convective heat transfer. However, on the top, the effects of wind velocity are still prevalent, and as such, the losses due to heat transfer from the top surface must be considered. The effect of wind velocity have been accounted by using the convective heat transfer coefficient expressed as (Palyvos, 2008),

$$h_{top} = 4.0V_{wind} + 7.4 \quad (4.3)$$

The simulation results of the PVT-SAH model for the convective heat transfer coefficient mentioned above are in good agreement with the experimental data for similar BIPV/T structure installed at the Varennes library building in Quebec, Canada.

The radiative heat transfer from the exposed surface (top) of the collector is dependent on the emissivity of the surface, and the temperature difference between the surface and the ambient. A lower emissivity helps to achieve higher outlet air temperatures which is desirable with the application of the SAH. To improve the thermal energy gain and reduce the top radiative heat transfer losses, a SAH with glazed top cover with emissivity of 0.3 is employed.

The fan consumption of the PVT-SAH is affected by the pressure drop across the air channel's length. This phenomenon can be expressed through following equations (Cengel YA et al., 2016):

$$\dot{W}_{fan} = \frac{\dot{W}_h}{\eta_{fan}\eta_{motor}} \quad (4.4)$$

Where \dot{W}_{fan} (kW) is the electrical fan power due to frictional pressure drop along the air channel, \dot{W}_h (kW) is the hydraulic fan power, η_{fan} is the fan efficiency, η_{motor} is the motor efficiency. The hydraulic fan power is defined as (Cengel YA et al., 2016):

$$\dot{W}_h = \dot{V}(\Delta P_k + \Delta P_f) \quad (4.5)$$

Where \dot{V} (m³/s) is the volumetric flow rate of air through the air channel, ΔP_k (Pa) is the kinetic pressure drop and ΔP_f (Pa) is the frictional pressure drop. The frictional pressure drop across the air channel is defined as:

$$\Delta P_f = \Delta P_M + \Delta P_m \quad (4.6)$$

Where ΔP_M is the major frictional pressure drop and ΔP_m is the minor frictional pressure drop. Amongst the different types of pressure drops, the most significant one contributing towards the rise in fan consumption in this study is the major frictional pressure drop, and it is defined as (Cengel YA et al., 2016):

$$\Delta P_M = \sum_{i=1}^n f_i \frac{L_i}{D_{Hi}} \frac{\rho V_{iavg}^2}{2} \quad (4.7)$$

Where f_i is the friction factor, L_i (m) is the length of the air channel, D_{Hi} (m) is the hydraulic diameter, ρ is the density of air, and V_{iavg} is the average air velocity through the air channel.

Desiccant dehumidifier, cooling unit, and a regenerative heat source are the main components of a Solid Desiccant Cooling (SDC) system. The pressure drop across the SDC system components should also be considered as higher flow rates can result in higher pressure drops, which is responsible for increased power consumption.

4.3.1 Equipment Sizing for Baseline Model

Based on the peak sensible and latent load of the retail store, the supply air flow rate and minimum fresh air ventilation requirements are calculated as per NBC of India and ASHRAE 90.1 (Bureau of Indian Standards (BIS), 2016)(ASHRAE Standard 90.1, 2016). The minimum fresh air required to maintain good indoor air quality in the store comes around 2 air changes per hour (ACH) (ASHRAE Standard 62.1, 2016). The integrated system works on recirculation mode which uses 25% outdoor air (approximately 2 ACH) and the rest of the room return air is recirculated at the inlet of the desiccant wheel. Operation of the integrated system is explained in the section 4.3.3.

Auxiliary heater, evaporative coolers and fans contribute to the integrated system's electricity consumption. The integrated system uses four fans – fresh air supply, room return, regeneration ambient air, and auxiliary heater fan. Total fan power allowance is calculated as per (ASHRAE Standard 90.1, 2016) which assumes 0.64 Watt per litre per second. The regeneration air setpoint

is taken as 70°C and a 1000 Watts auxiliary heater is employed to maintain this setpoint for the considered air flow rate. The desiccant wheel and evaporative coolers require nominal energy for rotors and water pumps which have been assumed as per literature.

4.3.2 PVT-SAH Description

The PVT-SAH system is spread over half (or 110 m²) of the total rooftop and inclined at an optimal angle of 13° (Chennai latitude). However, a lower angle can also be beneficial owing to the dominant diffused radiation during the monsoon season (high cloud cover). Table 6 illustrates the dimensions of the PVT-SAH system. The PVT collector's main purpose is to produce electricity and supplement the Solar Air Heater (SAH) with recovered thermal energy. On the other hand, the SAH is solely responsible for boosting the outlet air temperature going into the auxiliary heater. Therefore, an unglazed PVT collector (for easier heat dissipation from top) and a glazed SAH (to trap the heat) are used. The PVT-SAH system is series arrangement of these two components with a common air channel extending across the entire system. This system uses one fan to ensure continuous heat extraction through forced convection.

Component	Dimensions (m)	Area (m ²)
PVT	14 x 7	98
SAH	1.85 x 7	12.95
Total	15.85 x 7	110.95
Air Channel Height	0.06	-

Table 6 Dimensions of PVT-SAH for the baseline model

4.3.3 Integrated PVT-SAH assisted SDC system Operation

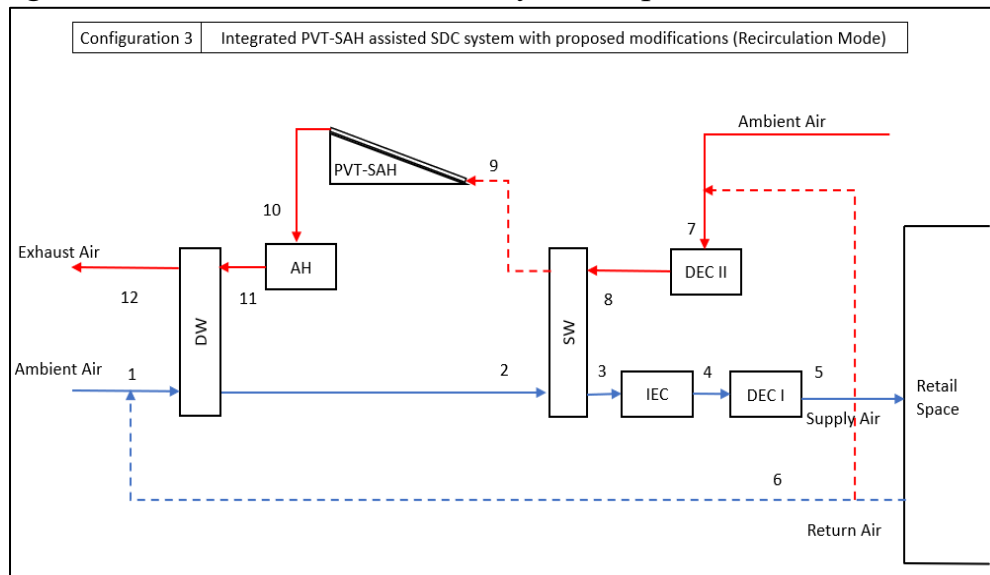


Figure 14 Integrated PVT-SAH assisted SDC system configuration 3 with proposed modifications (Recirculation Mode)

Figure 14 illustrates the schematic of the integrated system with the operation of the system on the supply side (1-6) in blue color and the regeneration side (7-12) in red color. On the supply side, the supply air, which is a mixture of small amount of fresh air and room return air (dotted blue line), undergoes dehumidification from 1-2 by passing through the Desiccant Wheel (DW). Then,

the heated and dehumidified supply air is sensibly cooled from 2-4 by passing through the Sensible Wheel (SW) and Indirect Evaporative Cooler (IEC). Then after, the cooled and dehumidified supply air undergoes evaporative cooling from 4-5 by passing through the Direct Evaporative Cooler (DEC I), to reach the desired setpoint conditions of the room. At last, the cooled and humidified supply air enters the retail store.

On the regeneration side, the regeneration air which is a mixture of ambient air and a small amount of room return air (dotted red line), undergoes evaporative cooling from 7-8 when it passes through the Direct Evaporative Cooler (DEC II). Then, the cooled and humidified regeneration air is sensible heated from 8-9 by passing through the SW. Then after, the regeneration air undergoes further sensible heating from 9-10 by passing through the air channel under the PVT-SAH system, boosting the temperature of regeneration air significantly. The heated regeneration air, then, passes through the Auxiliary Heater (AH) from 10-11; where the AH helps to raise the temperature in case it is lower than setpoint (70°C). The AH does not consume any energy if the regeneration air temperature exceeds 70°C. Finally, the regeneration air passes through the DW from 11-12; where the DW undergoes desorption at high temperature. The regeneration air is exhausted at the exit of the DW.

4.4 Retail store operation using Different Integrated System Configurations

4.4.1 Configuration 1: Typical integrated PVT-SAH assisted SDC system configuration in ventilation mode (100% fresh air)

This scenario represents the retail store operation using the integrated system configuration 1 in ventilation mode i.e. 100 % fresh air supply. This is the most common mode of operation of such a system making it a good baseline. Figure 15 illustrates the schematic of the integrated system configuration 1. The electrical and thermal energy gain through the PVT-SAH helps to fulfil SDC’s regeneration as well as AH energy requirements.

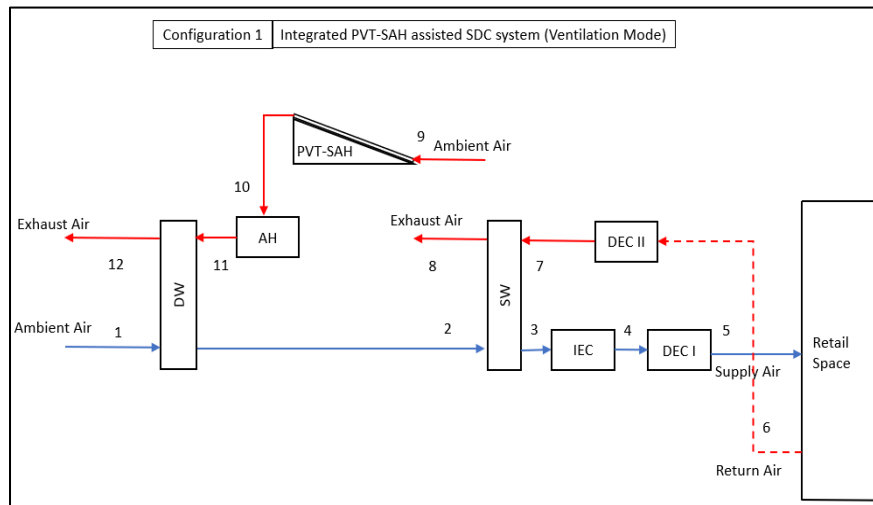


Figure 15 Typical integrated system configuration 1 in ventilation Mode

4.4.2 Configuration 2: Typical integrated PVT-SAH assisted SDC system configuration in recirculation mode

This scenario considers a typical PVT-SAH assisted SDC system operating in recirculation mode. Figure 16 illustrates the schematic of the integrated systems configuration 2. In this configuration, the air exiting from the sensible heat exchanger (Sensible Wheel, or SW) is exhausted, and ambient air is fed into the PVT-SAH on the regeneration side. Therefore, it should be noted that there is no direct interaction between the SW and the PVT-SAH in this configuration.

As can be seen in figures 15 and 16, both configurations 1 and 2 represent open exhaust air discharge type of arrangement for coupling the SW outlet with PVT-SAH inlet.

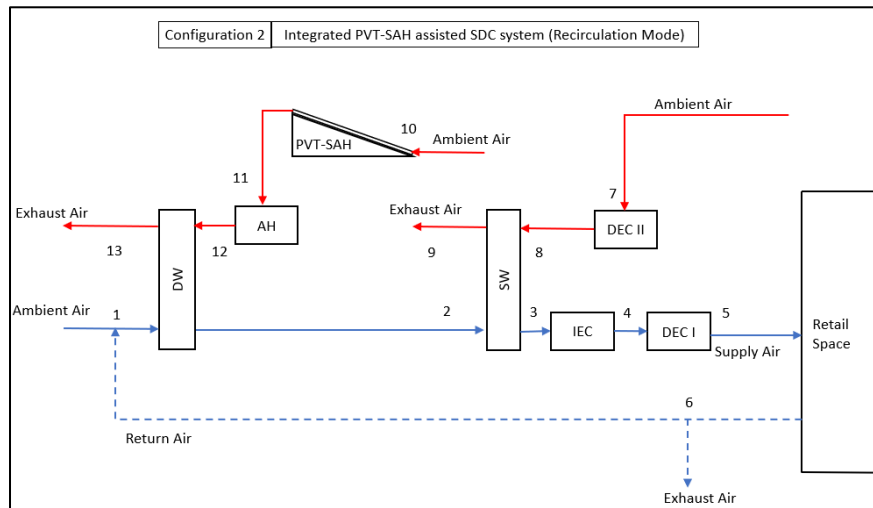


Figure 16 Typical integrated system configuration 2 in recirculation mode

4.4.3 Configuration 3: Existing integrated PVT-SAH assisted SDC system configuration in recirculation mode with proposed modifications

This scenario considers an existing integrated PVT-SAH assisted SDC system configuration 3 operating in recirculation mode with proposed modifications. Figure 17 illustrates the schematic of the integrated system configuration. In this configuration, the air exiting from the SW is fed into the PVT-SAH on the regeneration side. The overall thermal performance of the integrated system is expected to change because of this arrangement.

The configuration 3 represents close exhaust air discharge type of arrangement for coupling the SW outlet with PVT-SAH inlet.

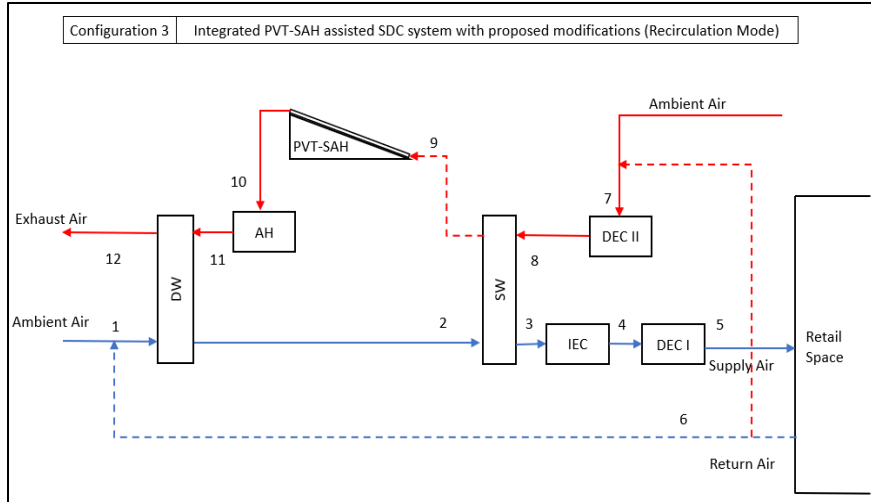


Figure 17 Existing integrated system configuration 3 in recirculation mode with proposed modifications

4.5 Sensitivity Analysis and Optimization Study

4.5.1 Sensitivity Analysis

A sensitivity analysis has been conducted for the integrated system configuration 3 to investigate the interaction between the design parameters (input variables) and the objective functions (output variables), and to identify the most influential parameters. Table 7 shows the original set of design parameters for the sensitivity analysis.

Collector area (m ²)	Collectors L/W ratio	PV covering factor	Channel height (m)	Mass flow rate (kg/s)
25	1.0	0.75	0.04	0.3
50	1.5	0.80	0.07	0.6
75	2.0	0.85	0.10	0.9
100	2.5			1.2

Table 7 Design Parameters for the Sensitivity Analysis

Following outputs related to the integrated PVT-SAH assisted SDC system are considered.

- Auxiliary heater energy consumption (kWh)
- PV electrical energy gain (kWh)
- PV surface temperature (°C)
- Solar air collector outlet temperature (°C)
- The temperature difference between 1. Overall collector inlet and outlet, 2. Solar air collector inlet and outlet (°C)
- PVT-SAH thermal energy gain (kWh)
- Electrical efficiency
- The pressure drop across the collector

4.5.1 Optimization Study

Next, a multi-objective optimization analysis is performed to accommodate the multi-criteria decision-making procedure for optimizing the PVT-SAH assisted SDC system.

Based on the sensitivity analysis, air mass flow rate, collector area and channel height are selected as the main design parameters for the optimization. More details on the reasons for this decision are discussed in chapter 5. The design parameters used in this optimization and their ranges are shown in Table 8.

Air mass flow rate (kg/s)	Collector area (m ²)	Channel height (m)
0.3	5	0.04
0.6	24	0.07
0.9	43	0.10
1.2	62	
1.5	81	
1.8	100	
2.1		

Table 8 Design Parameters for optimization

Multi-objective Genetic Algorithm (GA) optimization is used to maximize the annual PV electrical energy gain and minimize the AH energy consumption. Besides, the PV surface temperature is set as a constraint to minimize the impacts of high surface temperature. Table 9 shows details of the optimization. Table 10 illustrates the comparison of full factorial approach and optimization. The results of optimization converge after 7 generations with a total of 65 unique designs (cases) which is less in number than the full factorial approach.

Number of generations	50
Probability of directional cross-over	0.5
Probability of selection	0.05
Probability of mutation	0.1

Table 9 Details of Optimization

Approach	Total cases
Full factorial	576
Full factorial with sensitivity analysis	126
Optimization	65

Table 10 Comparison of full factorial with optimization

Chapter 5. Results and Discussions

This chapter is divided into three sections discussing all the simulation results of this study. The first section presents the energy performance results of the building (retail) and comparison of the three configurations. The second and third sections talk specifically about the investigation results related to the sensitivity analysis and optimization study.

5.1 Simulation Results of the Case Study

The building energy model representing a typical 4-story mixed-use building was simulated to understand the building energy demand with respect to the local building energy regulations. Initially, ideal air loads system was used to determine the annual energy performance of the building. The annual energy performance results show good agreement with the energy performance values of surveyed buildings in Chennai, India. These results are presented in Appendix B. Based on the three scenarios, results of the integrated PVT-SAH assisted SDC systems's energy performance and supply air characteristics are presented here. It should be noted that all the results in this section are presented as per the schedule hours (9:00 AM-5:00 PM) for the retail store.

5.1.1 PVT-SAH Energy Gain

Figures 18 and 19 illustrate the monthly PV electrical energy gain (kWh) and thermal energy gain (kWh). All the configurations show a typical trend for energy gain, primarily resulting from variation in the local GHI and cloud cover. The location analysis section (Chapter 4) briefly discusses Chennai's monthly GHI and average cloud coverage. The lower electrical energy gain in the summer months results mainly because of the low GHI and high cloud coverage during the monsoon season.

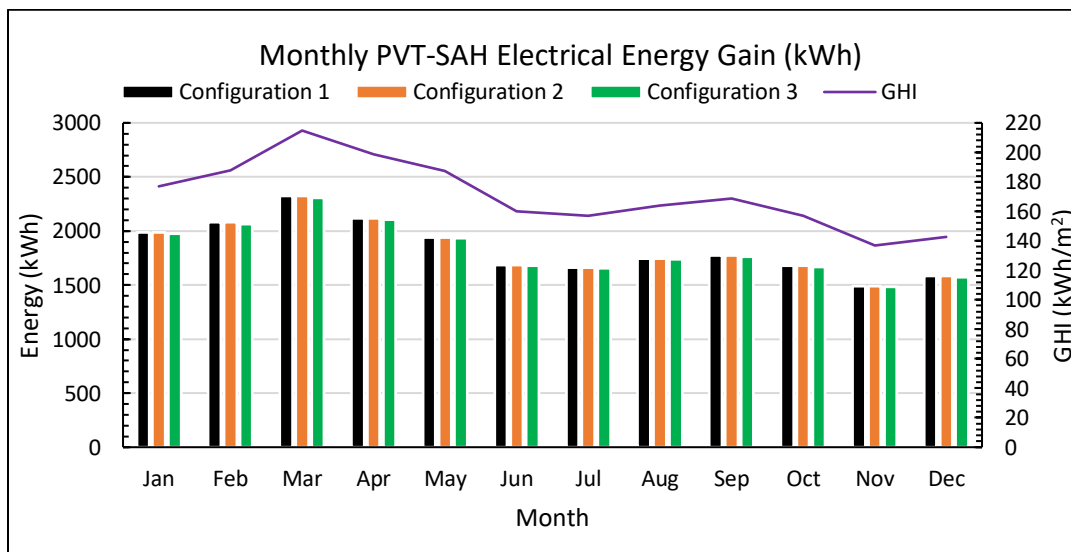


Figure 18 Monthly PVT-SAH Electrical Energy Gain (kWh)

All the configurations have almost identical PV electrical energy gain throughout the year. The monthly average PV surface temperature lies within the range of 42-53°C; however, maximum PV

surface temperature exceeds 70°C on several occasions which is undesirable. The thermal energy gain for configurations 1 and 2 is higher than configuration 3. The interaction between the Sensible Wheel (SW) and the PVT-SAH is responsible for the variation in thermal energy gain. Figure 20 illustrates the monthly average PVT-SAH inlet air temperature which helps to understand this phenomenon. Throughout the year, ambient air temperature is lower than SW outlet air temperature (6.57°C on an average). The thermal energy gain depends on the temperature difference between the inlet and the outlet of the PVT-SAH. In configurations 1 and 2 the inlet temperature is lower than configuration 3, resulting in higher thermal energy gain in configurations 1 and 2.

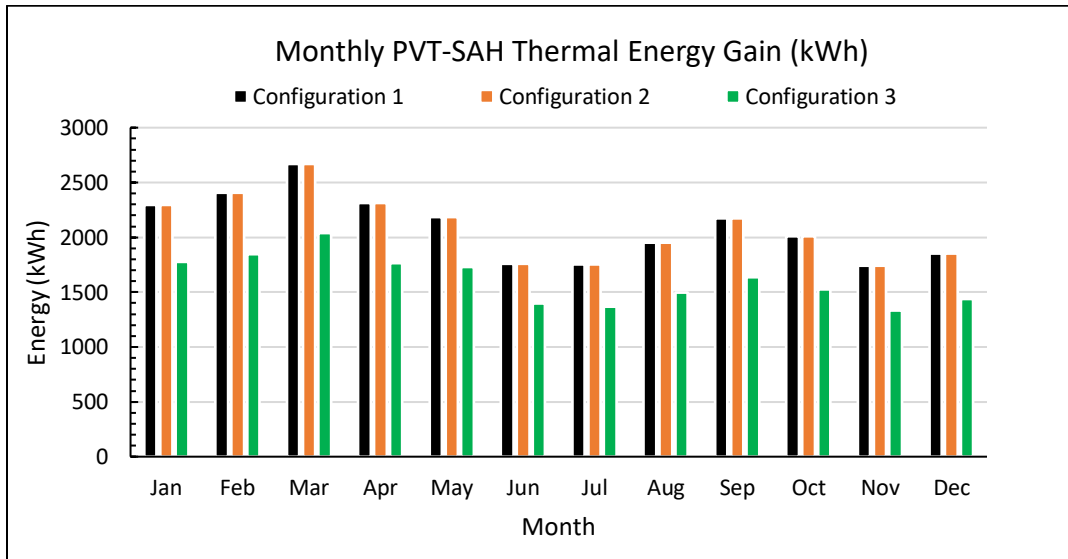


Figure 19 Monthly PVT-SAH Thermal Energy Gain (kWh)

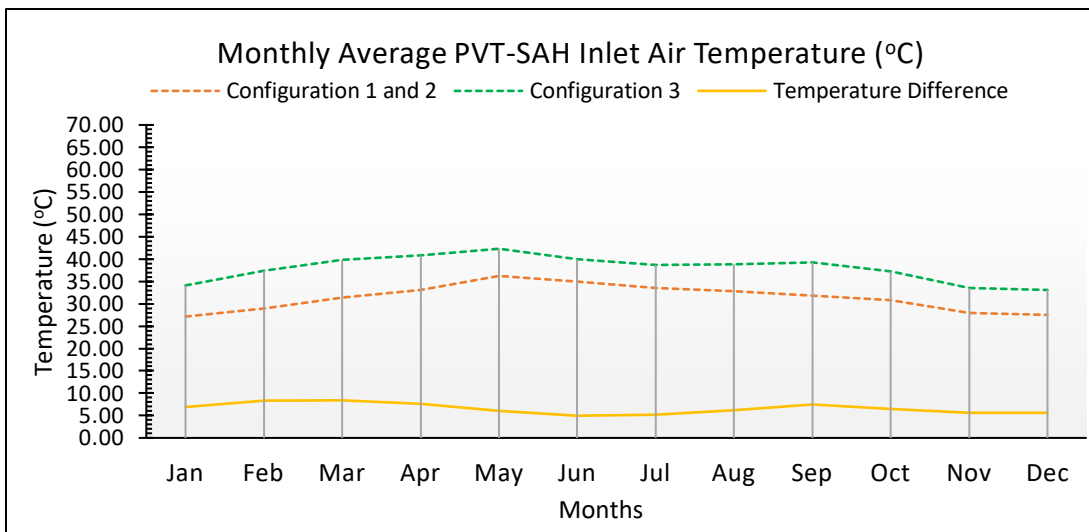


Figure 20 Monthly Average PVT SAH Inlet Air Temperature (°C)

However, this variation in thermal energy gain does not affect the PV electrical energy gain in any configuration, since the PV surface temperature does not change. At the same time, the PVT-SAH outlet air temperature remains almost the same. This is discussed in the next section.

Case	PV Electrical Gain (kWh/year)	PVT-SAH Thermal Gain (kWh/year)
Configuration 1	22,072	25,093
Configuration 2	22,072	25,093
Configuration 3	21,930	19,344

Table 11 Annual PVT SAH Electrical and Thermal Energy Gains

5.1.2 AH Energy Consumption

Figure 21 illustrates monthly average Solar Air Heater (SAH) inlet and outlet air temperatures. The temperature rise in the air because of SAH is same in all the configurations. The PVT-SAH can attain an additional 12°C temperature rise due to the addition of the SAH (without adversely affecting the PV electrical energy gain). Higher outlet air temperature from the PVT-SAH is necessary to reduce the auxiliary heater (AH) energy consumption. However, as mentioned in the previous section, the PV temperature exceeds 70°C in some instances which should be avoided. The optimization analysis will consider the effect of PV temperature by constraining it to 70°C.

Figure 22 illustrates the monthly AH energy (electrical) consumption in kWh for the three configurations. The AH energy consumption for all the three configurations is almost the same. A case of integrated system without PVT-SAH (only using AH) is considered to show the significant reduction (by 10 times) in AH energy consumption achieved in the three configurations. The temperature of inlet air to the AH significantly affects the capacity and subsequent energy consumption associated with the AH. The AH is switched off whenever inlet air temperature exceeds 70°C (setpoint). In the absence of a PVT-SAH, a higher capacity AH has to be used, resulting in higher energy consumption. These results point out the advantage and energy saving potential associated with the application of the PVT-SAH.

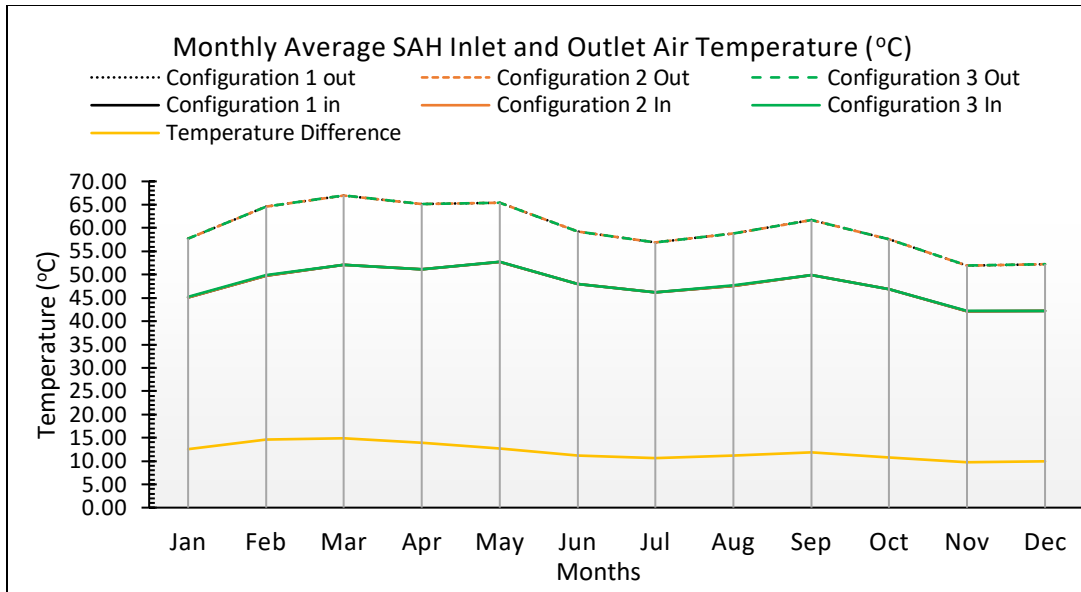


Figure 21 Monthly Average SAH Inlet and Outlet Air Temperature (°C)

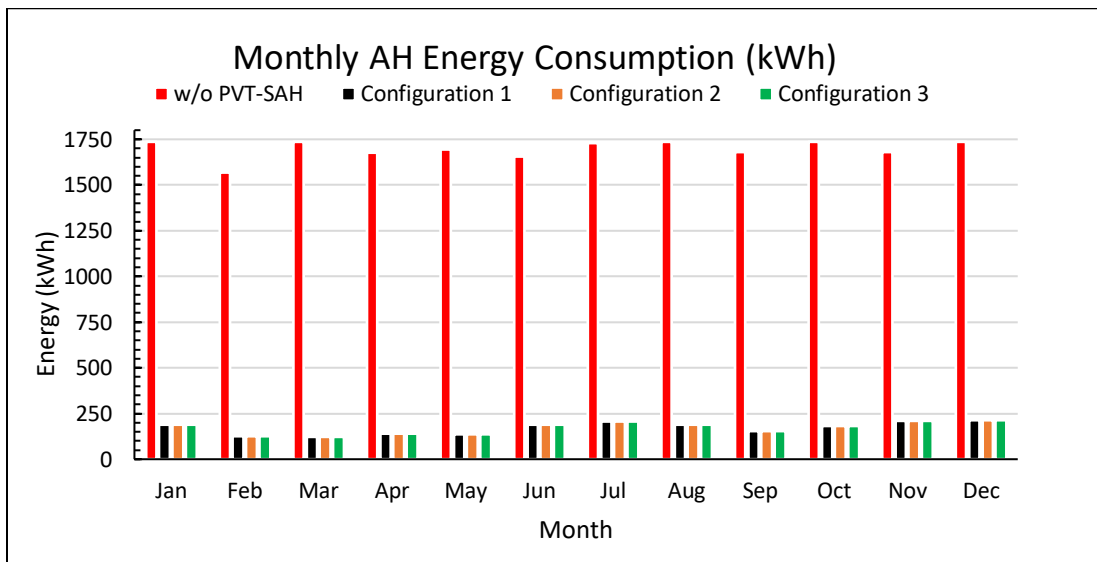


Figure 22 Monthly AH Energy Consumption (kWh)

Case	AH Energy (Electrical) Consumption (kWh/year)
W/O PVT-SAH	20,366
Configuration 1	2057
Configuration 2	2057
Configuration 3	2053

Table 12 Annual AH Energy Consumption

5.1.3 Thermal Coefficient of Performance

By definition, COP_{th} is a ratio of difference between room and supply air enthalpies to difference between AH and PVT-SAH outlet air enthalpies. Figure 23 illustrates the monthly average thermal

COP of the system for the three configurations. The COP_{th} is associated with the enthalpy of air passing through the system. In all the three configurations, the COP_{th} changes primarily because of change in the supply air enthalpy. This phenomenon is also discussed in Appendix C through steady state analysis of the integrated system configurations using psychrometric chart. The integrated PVT-SAH assisted SDC system configurations 1, 2 and 3 achieved annual average COP_{th} of 0.95, 1.90 and 2.23, respectively. The integrated system configuration 3 achieved better COP_{th} over the configurations 1 and 2, respectively, mainly because of two reasons.

First, portion of return air is mixed with ambient air and fed into the sensible wheel, improving the performance of the sensible wheel; in turn, offering better sensible cooling of supply air. At the same time, the closed loop between the sensible wheel exhaust and PVT-SAH inlet greatly helps to avoid wastage of processed air. Second, the recirculation cycle offers better control over the absolute humidity, reducing the supply air enthalpy, altogether resulting in a higher COP_{th} .

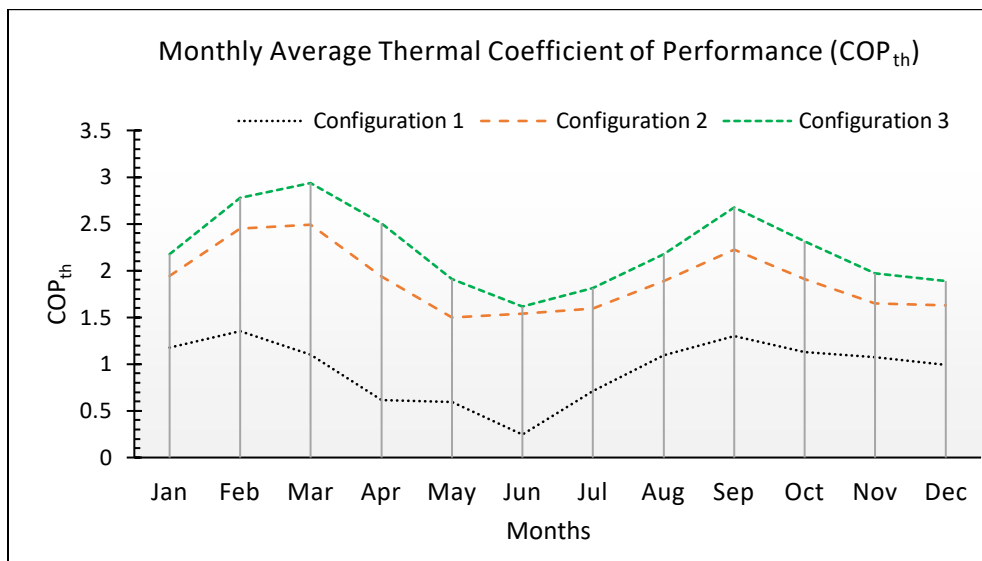


Figure 23 Monthly Average Thermal Coefficient of Performance (COP_{th})

5.1.4 Unmet Hours

Unmet hours (%) in this study are calculated as the percentage of the number of hours in the schedule during which the integrated system cannot maintain the room setpoint conditions of 26°C room air temperature and 65% room air relative humidity. As per the schedule 9:00 AM-5:00 PM, the total number of schedule hours are 2920. The unmet hours for the integrated system configurations 1, 2 and 3 were 23%, 18% and 12%, respectively.

Case	Unmet Hours (hours)	Unmet Hours (%)
Configuration 1	678	23
Configuration 2	519	18
Configuration 3	369	12

Table 13 Unmet Hours Comparison

Figures 24 and 25 illustrate the monthly average room air temperature and relative humidity achieved by the integrated system in the three configurations. It can be seen that the integrated system configuration 3 achieved better room air conditions in comparison with the other two configurations. As almost 75% of the return air is recirculated at the inlet of the Desiccant Wheel (DW), and owing to improved sensible cooling (through sensible wheel), the integrated system configuration 3 is able to cool and dehumidify the supply air more effectively.

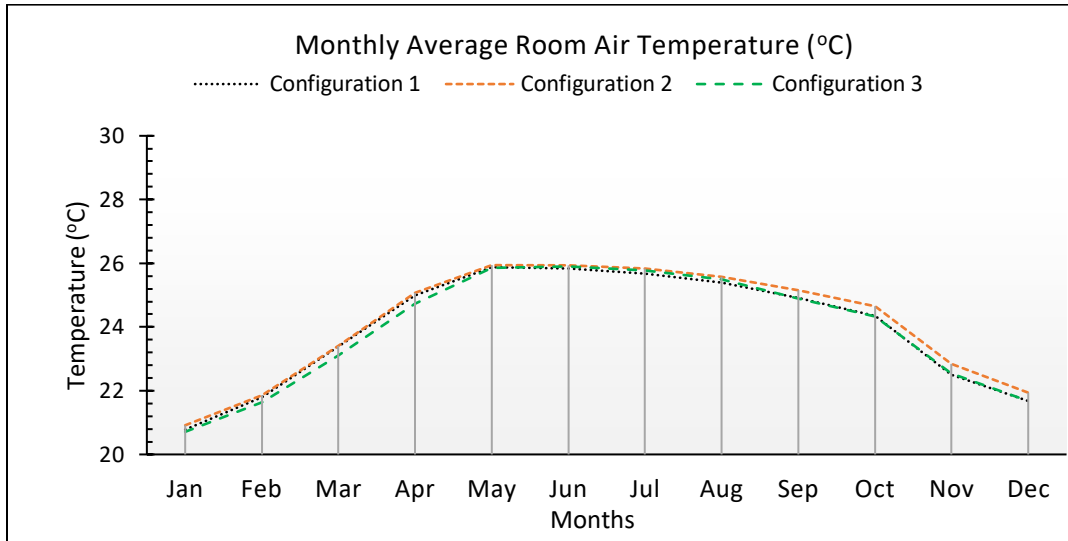


Figure 24 Monthly Average Room Air Temperature (°C)

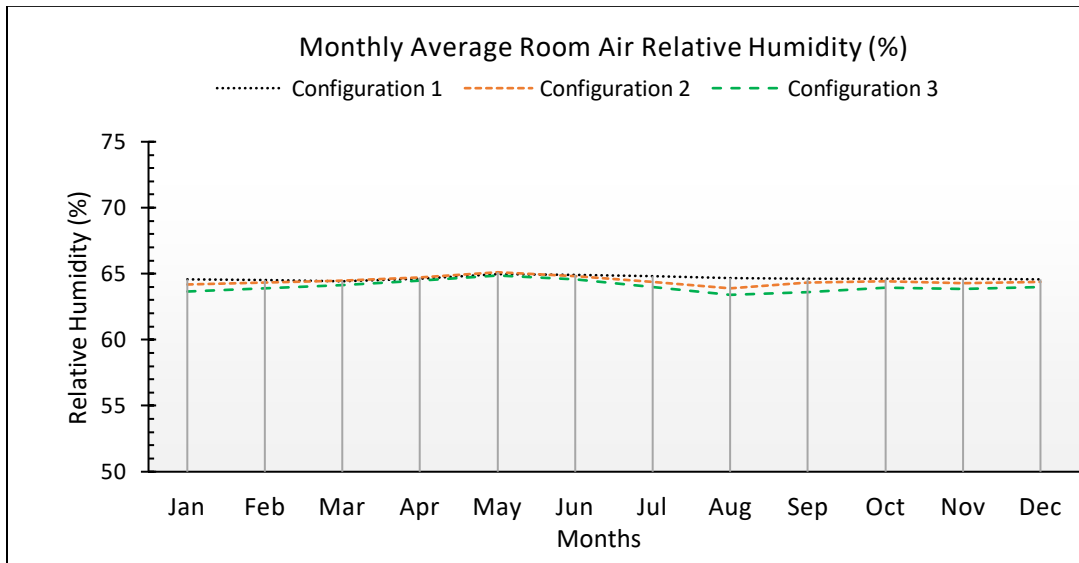


Figure 25 Monthly Average Room Relative Humidity (%)

5.1.5 Comparative Performance Improvement

Although the thermal energy gain of the PVT-SAH is reduced, the integrated system configuration 3 with proposed modifications offer better thermal coefficient of performance and reduced unmet hours without sacrificing the PVT-SAH electrical energy gain. More precisely, the integrated system configuration 3 achieved 135% and 18% improvement in COP_{th} and reduced the unmet

hours by 48% and 33% in comparison with the configurations 1 and 2. It should also be noted that the auxiliary heater energy consumption stays almost the same in all the configurations. Therefore, optimization study is conducted using the integrated system configuration 3 as a baseline. A comparison of performance improvements achieved by configuration 3 over configuration 1 and 2 is presented in Table 14.

Performance Indicators	Performance Improvement by Configuration 3 over	
	Configuration 1	Configuration 2
COP_{th}	135%	18%
Unmet Hours	48%	33%

Table 14 Comparison of Performance Improvements

The sensitivity analysis results, discussing the different design parameters that impact the performance of the integrated system is discussed in the next section.

5.2 Sensitivity Analysis Results

Figure 26 illustrates the impacts of the design parameters on all the different outputs of the integrated PVT-SAH assisted SDC system. As shown in the figure, air mass flow rate and collector area are the most dominating design parameters. Air mass flow rate significantly affects the AH energy consumption and PVT-SAH fan consumption, while the collector area plays a dominant role in the PVT-SAH electrical energy gain, and overall air temperature rise in the solar collector (PVT-SAH).

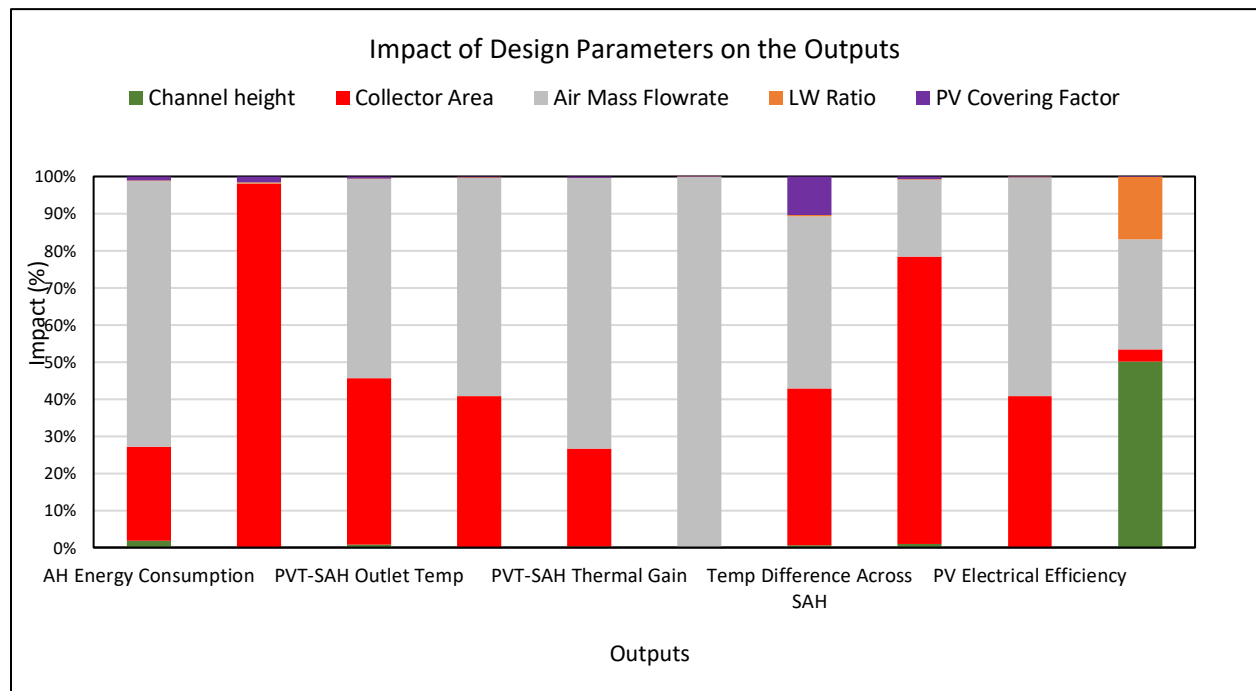


Figure 26 Impact of Design Parameters on the Outputs

The pressure drop is mainly affected by the variation of the channel height and the air mass flow rate. However, in this case, with low mass flow rate values, the pressure drop across the collector (PVT-SAH) is negligible. On the other hand, the PVT-SAH fan consumption is directly related to the pressure drop and air mass flow rate across the collector (PVT-SAH). As a result, the impact of channel height on the PVT-SAH fan consumption due to low air mass flow rate and negligible pressure drop is insignificant. As a result, the AH fan consumption is only affected by the air mass flow rate.

Therefore, for the optimization study, the channel height must be kept as low as possible to increase the heat transfer and collector (PVT-SAH) outlet air temperature as long as it satisfies the constraint for PV surface temperature ($<70^{\circ}\text{C}$).

The influence of the collector L/W ratio is only accountable for pressure drop calculation. For the objectives and range of inputs selected in this study, the L/W ratio can be neglected since, as discussed, the pressure drop across the collector will almost always be negligible.

The PVT collector cover emissivity was also initially included in the sensitivity analysis. However, for the selected range, the impact of this parameter on the objectives of this research was minimal. Hence a default low value for cover emissivity was assumed (glazed cover). The PV covering factor increases the Solar Air Heater (SAH) outlet temperature minimally but reduces the PVT-SAH electrical energy gain significantly. Since the electrical energy gain is considered to be higher grade energy than the thermal energy gain, a high PV covering factor was considered to ensure higher PVT-SAH electrical energy gain.

Based on the results of the sensitivity analysis, collector area (m^2), air mass flowrate (kg/s), and channel height (m) were selected for maximizing the PV electrical energy gain and minimizing the AH energy consumption. Also, PV surface temperature of less than 70°C has been taken as a constraint for the optimization study.

5.3 Optimization Study Results

Figure 27 illustrates a bubble plot showing the design space for maximizing the PV electrical energy gain and minimizing the AH energy consumption, based on the selected input design parameters and constraint. It can be seen in figure 27 that the PV electrical energy gain is affected predominantly by the collector area covering the PV modules. Through this figure, the amount of PV electrical energy gain can easily be discretized and grouped based on the variation in collector area. This behavior supports the conclusion from sensitivity analysis that air mass flow rate and channel height do not considerably affect the PV electrical energy gain in comparison to the variation in the collector area.

The air mass flow rate primarily affects the AH energy consumption. This effect is different for various collector areas. Figure 27 also shows that the changes in AH consumption with the distinct air mass flow rate is not as significant as changes in PV electrical energy gain with various collector areas. However, for higher collector areas, the AH consumption is more sensitive to the air mass flow rate of the collector. Therefore, for higher collector areas, it is essential to manage and control the operation of the system more cautiously.

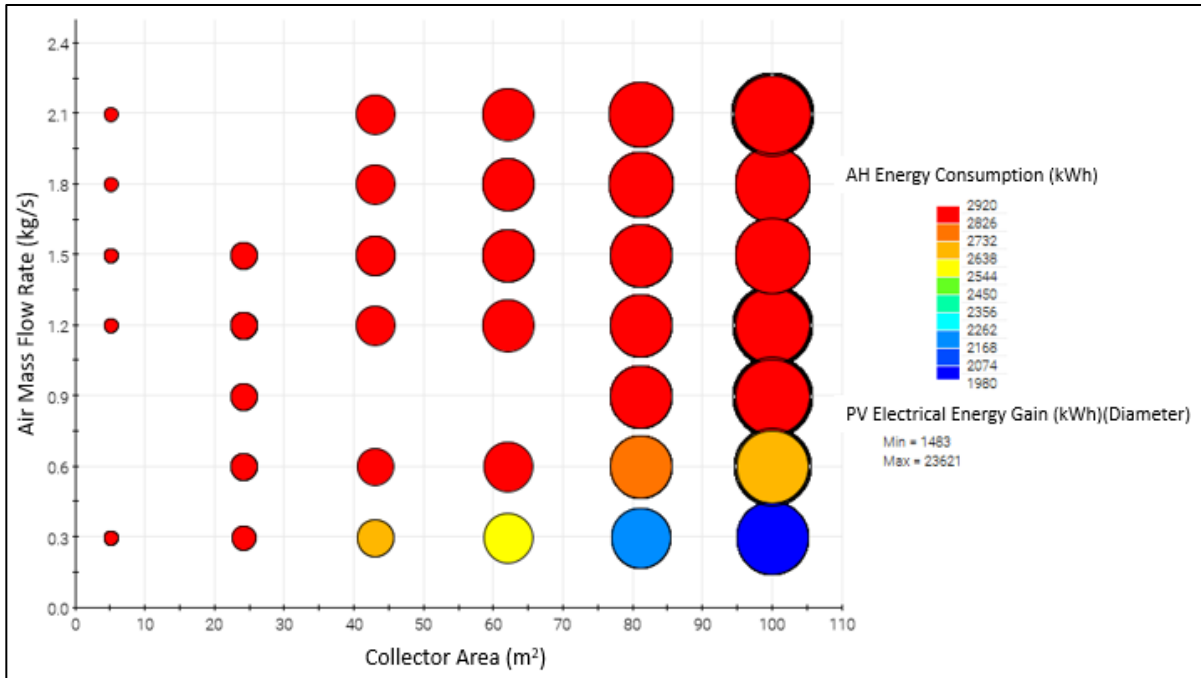


Figure 27 Bubble plot showing the design space for selected design parameters

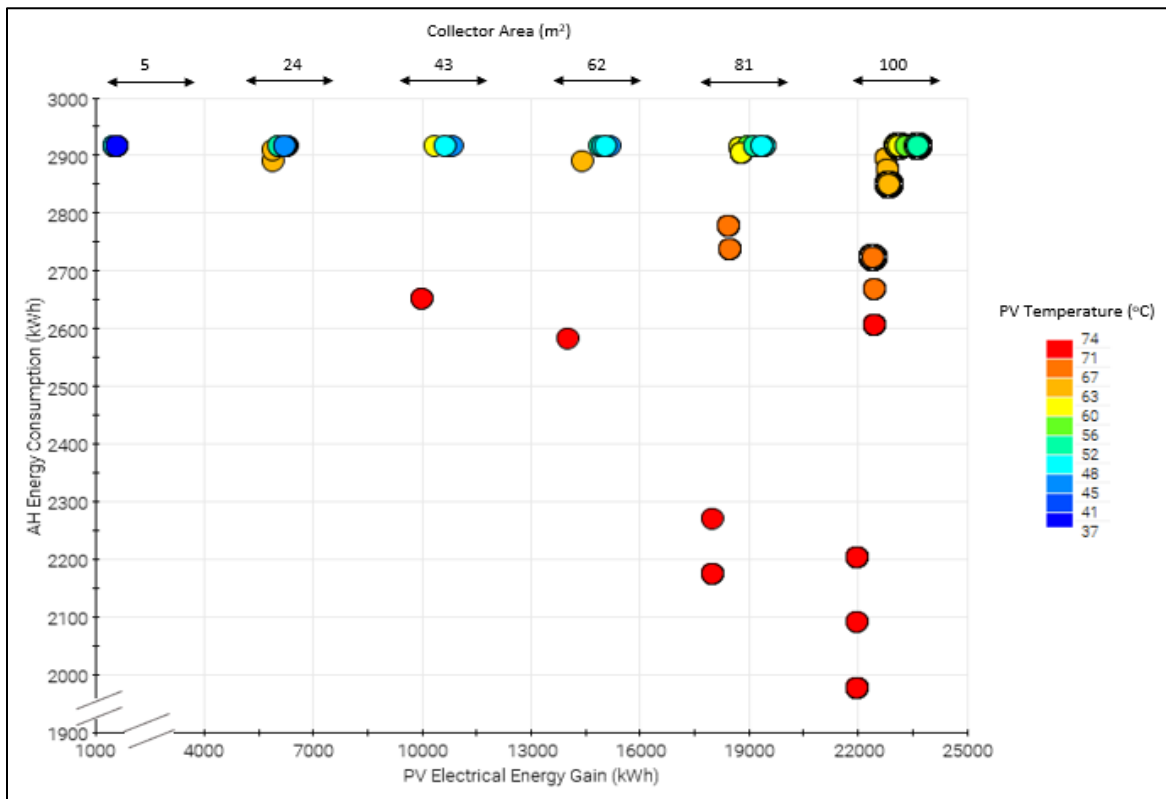


Figure 28 Bubble plot showing the Pareto Front between the Objective functions

Higher outlet air temperature from the PVT-SAH is necessary to reduce the AH energy consumption. However, higher outlet air temperature results in lower PV electrical energy gain.

Due to this conflicting relationship between the objectives of this study, a Pareto front is formed between them. Figure 28 illustrates a bubble plot showing the Pareto front between the objective functions, meaning that higher PV electrical energy gain will have higher AH energy consumption. It should be noted that all the design solutions consider the instantaneous maximum value of constraint temperature to decide the feasibility of the design. However, in reality, this can be misleading as the frequency of the event when constraint temperature is exceeded happens rarely throughout the year barring a few occasions. As such, although a few design solutions are deemed unfeasible, some of these designs can still be selected.

In this study, air mass flowrates between 0.3 kg/s – 2.1 kg/s have been considered, corresponding to an average air velocity inside the air channel between 0.57 m/s – 4.0 m/s. It is observed that lower channel height and lower average air velocities result in lower AH energy consumption. However, the AH energy consumption doesn't show any significant change beyond average air velocities of 2 m/s. Besides, while designing the PVT-SAH assisted SDC system, it should be noted that the air mass flow rate can significantly impact the integrated system's thermal energy gain and thermal coefficient of performance. Therefore, controlling the air mass flow rate and operation of the system in real-time condition will definitely improve the integrated system's performance.

Assuming daytime operation and higher collector areas, the PVT-SAH assisted SDC system offers surplus electrical energy gains since auxiliary heater is the biggest contributor towards energy consumption.

When more than one design parameter is considered (collector area and air mass flow rate), the PV electrical energy gain and AH energy consumption have a conflicting relationship. As the flow in the channel increases, the thermal energy gain rises, but the PVT-SAH collector outlet temperature is reduced, resulting in an increase in the AH energy consumption. In contrast, a rise in the PVT-SAH thermal energy gain improves the PV electrical energy gain.

For instance, a system with a lower collector area will have a significantly lower electrical energy gain (**approximately 22,000 kWh lower**) in comparison to a system with a high collector area. However, the variation in the collector area does not show a significant change in the AH energy consumption (**maximum change of 1000 kWh**). This correlation is particularly important as the collector area becomes the most critical parameter when higher electrical energy gain is desired. Whereas the air mass flow rate and to a minor extent, the collector area are important when the objective is to minimize the AH energy consumption. Figure 29 and 30 illustrate a parallel plot which helps to understand this phenomenon. In the parallel plot, all the lines represent different designs based on a combination of values for collector area, air mass flowrate and channel height. The green and yellow lines represent feasible and unfeasible designs, respectively. The parallel plot helps to visualize and understand the variation in outputs with the variation in input design parameters. Appendix D presents more parallel plots illustrating all the different designs and variation in the values of the objective functions in relation to different collector areas.

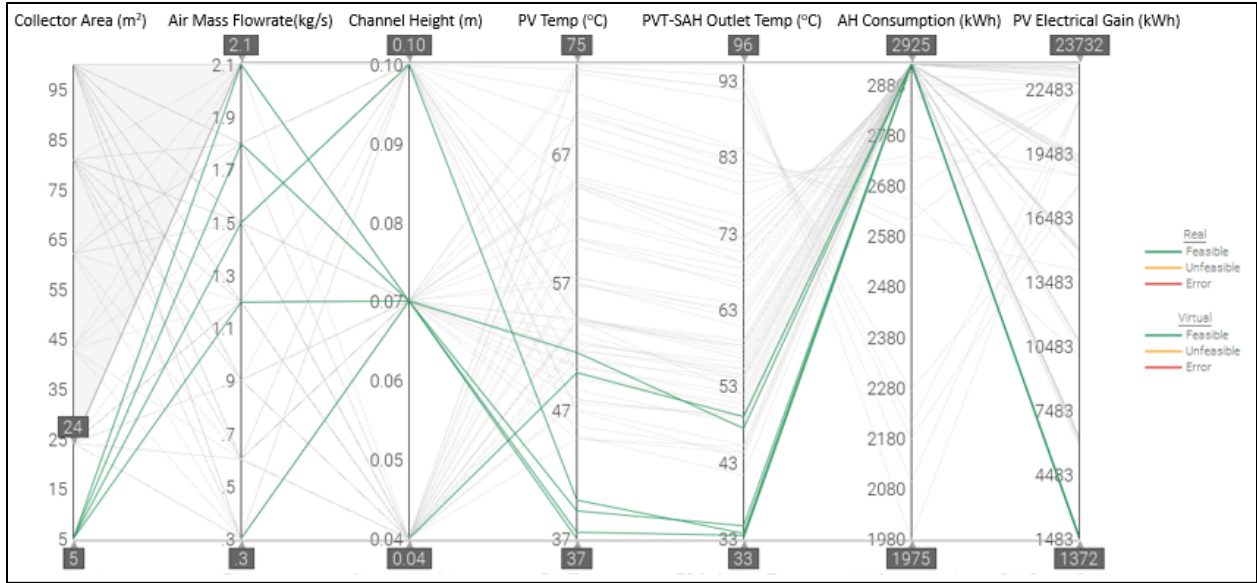


Figure 29 Parallel Plot showing variation in the objective functions for small collector areas

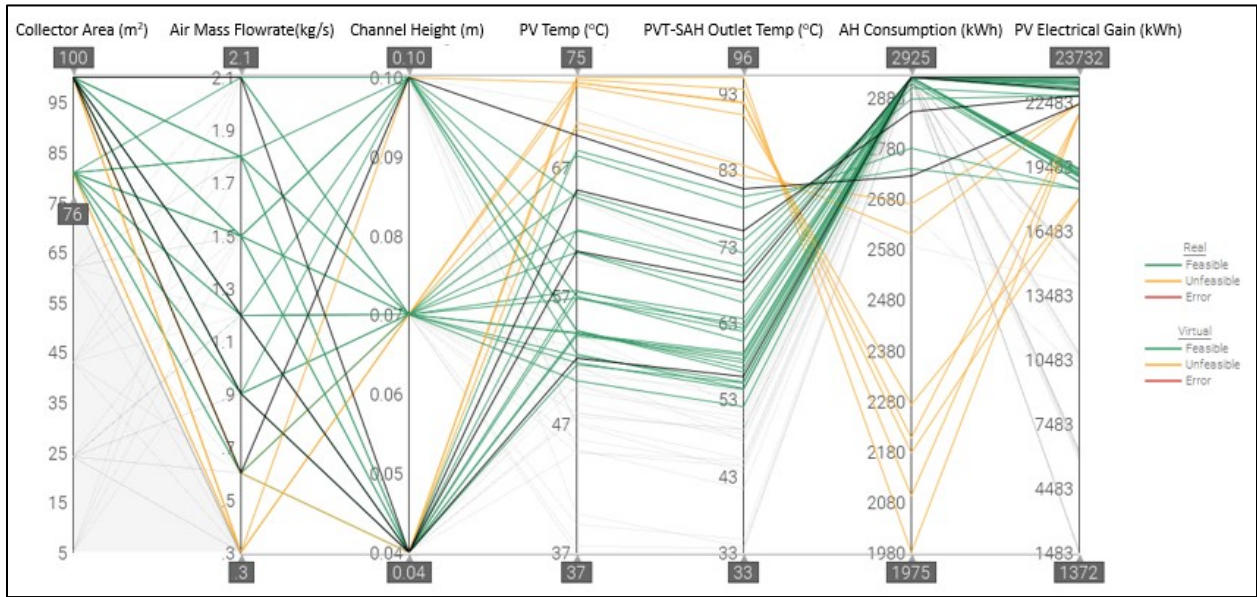


Figure 30 Parallel Plot showing variation in the objective functions for large collector areas

Chapter 6. Conclusions

In this research, a simulation-based investigation of three configurations of an integrated Photovoltaic Thermal Solar Air Heater (PVT-SAH) assisted Solid Desiccant Cooling (SDC) system was conducted. Some modifications to an existing PVT-SAH assisted SDC system configuration were proposed.

- The integrated system configuration with proposed modifications (Figure 15) achieved **135%** and **18%** improvement in thermal coefficient of performance (COP_{th}) over configurations 1 (Figure 16) and 2 (Figure 17), respectively.
- The improvement in COP_{th} was achieved without sacrificing the PV electrical energy gain and AH energy consumption of the integrated system.
- The integrated system configuration with proposed modifications (Figure 15) achieved **48%** and **33%** reduction in unmet hours in over configurations 1 (Figure 16) and 2 (Figure 17), respectively.

The integrated system configuration 3 with proposed modifications was selected as baseline for the sensitivity analysis and multi-objective optimization study to maximize the PV electrical energy gain and minimize the AH energy consumption.

- As per the sensitivity analysis, the collector area, air mass flow rate, and channel height are the most important design parameters.
- The results of the optimization study show a pareto front between the two objectives, meaning an integrated PVT-SAH assisted SDC system with a higher PV electrical energy gain will incur a higher AH energy consumption.
- It was concluded that the AH energy consumption is more sensitive to the air mass flow rate for larger collector areas. In contrast, the PV electrical energy gain is more sensitive to the collector areas.

The successful application of an integrated PVT-SAH assisted SDC system will depend on the available roof area to accommodate the PVT-SAH (collector area) and the air mass flowrate necessary to provide the desired outlet air temperature for the SDC system operation. Both of these design parameters impact the PV electrical energy gain and AH energy consumption. This research provides assistance to identify the best design solutions based on the previously mentioned design parameters for optimal performance of an integrated system in hot and humid climates.

6.1 Contributions

- Through this research some modifications to an existing configuration of an integrated PVT-SAH assisted SDC system for building space cooling application were developed. These modifications helped to improve the thermal coefficient of performance and reduce the unmet hours associated with the integrated system.
- A design methodology for integration and building application of PVT-SAH assisted SDC system in hot and humid climates was developed.

Appendix A presents detailed information of the publications based on this work.

6.2 Future Work Opportunities

- Investigation of application of two stage cycle and additional components to the existing integrated system.
- Multi-objective optimization of the integrated system for net-electricity gains and annualised relative cash flow.
- Investigation of a hybrid PVT-SAH assisted SDC system coupled with a conventional cooling technology (VCR system) for hot and humid climates.
- Development of a control strategy for an integrated system to improve the thermal comfort conditions and associated electricity consumption.

References

- Ahmed, M. H., Kattab, N. M., & Fouad, M. (2005). Evaluation and optimization of solar desiccant wheel performance. *Renewable Energy*, 30(3), 305–325. <https://doi.org/https://doi.org/10.1016/j.renene.2004.04.010>
- Al-Waeli, A. H. A., Sopian, K., Kazem, H. A., & Chaichan, M. T. (2017). Photovoltaic/Thermal (PV/T) systems: Status and future prospects. *Renewable and Sustainable Energy Reviews*, 77, 109–130. <https://doi.org/https://doi.org/10.1016/j.rser.2017.03.126>
- ASHRAE Standard 169. (2013). *Climatic Data for Building Design Standards*. [https://ashrae.iwrapper.com/ViewOnline/Standard_90.1-2016_\(IP\)](https://ashrae.iwrapper.com/ViewOnline/Standard_90.1-2016_(IP))
- ASHRAE Standard 55. (2013). *Thermal Environmental Conditions for Human Occupancy*. https://ashrae.iwrapper.com/ViewOnline/Standard_55-2013
- ASHRAE Standard 62.1. (2016). *Ventilation for Acceptable Indoor Air Quality*. https://ashrae.iwrapper.com/ViewOnline/Standard_62.1-2016
- ASHRAE Standard 90.1. (2016). *Energy Standard for Buildings Except Low-Rise Residential Buildings*. [https://ashrae.iwrapper.com/ViewOnline/Standard_90.1-2016_\(IP\)](https://ashrae.iwrapper.com/ViewOnline/Standard_90.1-2016_(IP))
- Aste, N., Chiesa, G., & Verri, F. (2008). Design, development and performance monitoring of a photovoltaic-thermal (PVT) air collector. *Renewable Energy*, 33(5), 914–927. <https://doi.org/https://doi.org/10.1016/j.renene.2007.06.022>
- Athienitis, A. K., Bambara, J., O’Neill, B., & Faille, J. (2011). A prototype photovoltaic/thermal system integrated with transpired collector. *Solar Energy*, 85(1), 139–153. <https://doi.org/https://doi.org/10.1016/j.solener.2010.10.008>
- Bureau of Energy Efficiency (BEE) India. (2016). *Design Guidelines for Energy-Efficient Multi-Storey Residential Buildings*.
- Bureau of Energy Efficiency (BEE) India. (2018). *Energy Conservation Building Code for Residential Buildings*. Bureau of Energy Efficiency (BEE) India.
- Bureau of Indian Standards (BIS). (2016). *National Building Code of India*. <http://archive.org/details/nationalbuilding01>
- Cengel YA, Turner RH, & Cimbala JM. (2016). *Fundamentals of Thermal-Fluid Sciences* (5th editio). McGraw-Hill Education.
- Central Electricity Authority. (2013). *Growth of electricity sector in India from 1947-2013*.
- Chow, T. T. (2010). A review on photovoltaic/thermal hybrid solar technology. *Applied Energy*, 87(2), 365–379. <https://doi.org/https://doi.org/10.1016/j.apenergy.2009.06.037>
- Chung, J. D., & Lee, D.-Y. (2011). Contributions of system components and operating conditions to the performance of desiccant cooling systems. *International Journal of Refrigeration*, 34(4), 922–927. <https://doi.org/https://doi.org/10.1016/j.ijrefrig.2011.03.003>
- Daou, K., Wang, R. Z., & Xia, Z. Z. (2006). Desiccant cooling air conditioning: a review.

- Renewable and Sustainable Energy Reviews*, 10(2), 55–77.
<https://doi.org/https://doi.org/10.1016/j.rser.2004.09.010>
- Deru, M., Field, K., Studer, D., Benne, K., Griffith, B., Torcellini, P., Liu, B., Halverson, M., Winiarski, D., Rosenberg, M., Yazdanian, M., Huang, J., & Crawley, D. (2011). *U.S. Department of Energy Commercial Reference Building Models of the National Building Stock*. <https://doi.org/10.2172/1009264>
- Duffie, J. A., & Beckman, W. A. T. A.-T. T.-. (2013). *Solar engineering of thermal processes LK* - <https://concordiauniversity.on.worldcat.org/oclc/836402985> (4th ed. NV). Wiley.
http://www.123library.org/book_details/?id=97363
- Dunkle, R. V. (1965). A method of solar air conditioning. *Mech Chem Eng Trans*, 1, 73–78.
- Eicker, U. (2014). Solar Cooling. In *Energy Efficient Buildings with Solar and Geothermal Resources* (pp. 297–417). <https://doi.org/doi:10.1002/9781118707050.ch5>
- Eicker, U., Schneider, D., Schumacher, J., Ge, T., & Dai, Y. (2010). Operational experiences with solar air collector driven desiccant cooling systems. *Applied Energy*, 87(12), 3735–3747. <https://doi.org/https://doi.org/10.1016/j.apenergy.2010.06.022>
- El-Sebaili, A. A., & Al-Snani, H. (2010). Effect of selective coating on thermal performance of flat plate solar air heaters. *Energy*, 35(4), 1820–1828.
<https://doi.org/https://doi.org/10.1016/j.energy.2009.12.037>
- Fan, W., Kokogiannakis, G., & Ma, Z. (2018). A multi-objective design optimisation strategy for hybrid photovoltaic thermal collector (PVT)-solar air heater (SAH) systems with fins. *Solar Energy*, 163, 315–328. <https://doi.org/https://doi.org/10.1016/j.solener.2018.02.014>
- Fan, W., Kokogiannakis, G., & Ma, Z. (2019). Integrative modelling and optimisation of a desiccant cooling system coupled with a photovoltaic thermal-solar air heater. *Solar Energy*, 193, 929–947. <https://doi.org/10.1016/j.solener.2019.10.030>
- Farshchimonfared, M., Bilbao, J. I., & Sproul, A. B. (2015). Channel depth, air mass flow rate and air distribution duct diameter optimization of photovoltaic thermal (PV/T) air collectors linked to residential buildings. *Renewable Energy*, 76, 27–35.
<https://doi.org/https://doi.org/10.1016/j.renene.2014.10.044>
- Florides, G. A., Kalogirou, S. A., Tassou, S. A., & Wrobel, L. C. (2002). Modelling and simulation of an absorption solar cooling system for Cyprus. *Solar Energy*, 72(1), 43–51.
[https://doi.org/https://doi.org/10.1016/S0038-092X\(01\)00081-0](https://doi.org/https://doi.org/10.1016/S0038-092X(01)00081-0)
- Florschuetz, L. W. (1979). Extension of the Hottel-Whillier model to the analysis of combined photovoltaic/thermal flat plate collectors. *Solar Energy*, 22(4), 361–366.
[https://doi.org/https://doi.org/10.1016/0038-092X\(79\)90190-7](https://doi.org/https://doi.org/10.1016/0038-092X(79)90190-7)
- Flycarpet. (2020). *Psychrometric Chart*. <http://www.flycarpet.net/en/PsyOnline>
- Fong, K. F., Chow, T. T., Lee, C. K., Lin, Z., & Chan, L. S. (2010). Comparative study of different solar cooling systems for buildings in subtropical city. *Solar Energy*, 84(2), 227–244. <https://doi.org/https://doi.org/10.1016/j.solener.2009.11.002>

- Ge, T. S., Dai, Y. J., & Wang, R. Z. (2014). Review on solar powered rotary desiccant wheel cooling system. *Renewable and Sustainable Energy Reviews*, 39, 476–497. <https://doi.org/https://doi.org/10.1016/j.rser.2014.07.121>
- Global Alliance for Buildings and Construction. (2016). *Global Roadmap towards low-GHG and resilient buildings*. <https://www.buildup.eu/en/practices/publications/global-roadmap-towards-low-ghg-and-resilient-buildings-0>
- Gommed, K., & Grossman, G. (2007). Experimental investigation of a liquid desiccant system for solar cooling and dehumidification. *Solar Energy*, 81(1), 131–138. <https://doi.org/https://doi.org/10.1016/j.solener.2006.05.006>
- Guo, J., Lin, S., Bilbao, J. I., White, S. D., & Sproul, A. B. (2017). A review of photovoltaic thermal (PV/T) heat utilisation with low temperature desiccant cooling and dehumidification. *Renewable and Sustainable Energy Reviews*, 67, 1–14. <https://doi.org/https://doi.org/10.1016/j.rser.2016.08.056>
- He, W., Barzinjy, A. A., Khanmohammadi, S., Shahsavari, A., Moghimi, M. A., & Afrand, M. (2020). Multi-objective optimization of a photovoltaic thermal-compound sensible rotary heat exchanger system using exergo-economic and enviro-economic approaches. *Journal of Environmental Management*, 254, 109767. <https://doi.org/https://doi.org/10.1016/j.jenvman.2019.109767>
- Henning, H.-M. (2007). Solar assisted air conditioning of buildings – an overview. *Applied Thermal Engineering*, 27(10), 1734–1749. <https://doi.org/https://doi.org/10.1016/j.applthermaleng.2006.07.021>
- IEA. (2018). *The Future of Cooling*. <https://www.iea.org/reports/the-future-of-cooling>
- IEA. (2019a). *Southeast Asia Energy Outlook*. <https://www.iea.org/reports/southeast-asia-energy-outlook-2019>
- IEA. (2019b). *The Critical Role of Buildings*. <https://www.iea.org/reports/the-critical-role-of-buildings>
- IEA. (2019c). *World Energy Outlook*. <https://www.iea.org/reports/world-energy-outlook-2019>
- Jani, D. B., Mishra, M., & Sahoo, P. K. (2016). Solid desiccant air conditioning – A state of the art review. *Renewable and Sustainable Energy Reviews*, 60, 1451–1469. <https://doi.org/https://doi.org/10.1016/j.rser.2016.03.031>
- Kruglov, O., Rounis, E., Athienitis, A., Lee, B., Bagchi, A., Ge, H., & Stathopoulos, T. (2018). *Modular Rooftop Building-Integrated Photovoltaic/Thermal Systems for Low-Rise Buildings in India*. <https://doi.org/10.18086/eurosun2018.06.12>
- La, D., Dai, Y. J., Li, Y., Wang, R. Z., & Ge, T. S. (2010). Technical development of rotary desiccant dehumidification and air conditioning: A review. *Renewable and Sustainable Energy Reviews*, 14(1), 130–147. <https://doi.org/https://doi.org/10.1016/j.rser.2009.07.016>
- Li, H., Dai, Y. J., Li, Y., La, D., & Wang, R. Z. (2011). Experimental investigation on a one-rotor two-stage desiccant cooling/heating system driven by solar air collectors. *Applied Thermal Engineering*, 31(17), 3677–3683.

<https://doi.org/https://doi.org/10.1016/j.applthermaleng.2011.01.018>

- Li, H., Dai, Y. J., Li, Y., La, D., & Wang, R. Z. (2012). Case study of a two-stage rotary desiccant cooling/heating system driven by evacuated glass tube solar air collectors. *Energy and Buildings*, 47, 107–112. <https://doi.org/https://doi.org/10.1016/j.enbuild.2011.11.035>
- Li, Z. X., Shahsavari, A., Al-Rashed, A. A. A. A., Kalbasi, R., Afrand, M., & Talebizadehsardari, P. (2019). Multi-objective energy and exergy optimization of different configurations of hybrid earth-air heat exchanger and building integrated photovoltaic/thermal system. *Energy Conversion and Management*, 195, 1098–1110. <https://doi.org/https://doi.org/10.1016/j.enconman.2019.05.074>
- Mateus, T., & Oliveira, A. C. (2009). Energy and economic analysis of an integrated solar absorption cooling and heating system in different building types and climates. *Applied Energy*, 86(6), 949–957. <https://doi.org/https://doi.org/10.1016/j.apenergy.2008.09.005>
- Mazzei, P., Minichiello, F., & Palma, D. (2002). Desiccant HVAC systems for commercial buildings. *Applied Thermal Engineering*, 22(5), 545–560. [https://doi.org/https://doi.org/10.1016/S1359-4311\(01\)00096-5](https://doi.org/https://doi.org/10.1016/S1359-4311(01)00096-5)
- Mei, L., Infield, D., Eicker, U., Loveday, D., & Fux, V. (2006). Cooling potential of ventilated PV façade and solar air heaters combined with a desiccant cooling machine. *Renewable Energy*, 31(8), 1265–1278. <https://doi.org/https://doi.org/10.1016/j.renene.2005.06.013>
- National Disaster Management Authority. (2013). *Seismic Vulnerability Assessment of Building Types in India*.
- Palyvos, J. A. (2008). A survey of wind convection coefficient correlations for building envelope energy systems' modeling. *Applied Thermal Engineering*, 28(8), 801–808. <https://doi.org/https://doi.org/10.1016/j.applthermaleng.2007.12.005>
- Pantic, S., Candanedo, L., & Athienitis, A. K. (2010). Modeling of energy performance of a house with three configurations of building-integrated photovoltaic/thermal systems. *Energy and Buildings*, 42(10), 1779–1789. <https://doi.org/https://doi.org/10.1016/j.enbuild.2010.05.014>
- Pennington, N. (1955). *Humidity changer for air conditioning* (Patent No. USA patent no. 2,700,537).
- Poles, S. (2003). *MOGA-II An improved Multi-Objective Genetic Algorithm*.
- Reddy, M. J., & Kumar, D. N. (2015). Elitist-Mutated Multi-Objective Particle Swarm Optimization for Engineering Design. *Encyclopedia of Information Science and Technology, Third Edit*, 3534–3545.
- Reinhart, C. (2014). The Source, in: Stein, R. (Ed.). In *Daylighting Handbook I* (pp. 39–61).
- Sahlot, M., & Riffat, S. B. (2016). Desiccant cooling systems: a review. *International Journal of Low-Carbon Technologies TA - TT -*, ctv032. <https://doi.org/10.1093/ijlct/ctv032> LK - <https://concordiauniversity.on.worldcat.org/oclc/5978501164>
- Shahsavari, A., & Khanmohammadi, S. (2019). Feasibility of a hybrid BIPV/T and thermal wheel

- system for exhaust air heat recovery: Energy and exergy assessment and multi-objective optimization. *Applied Thermal Engineering*, 146, 104–122.
<https://doi.org/https://doi.org/10.1016/j.applthermaleng.2018.09.101>
- Shukla, Y., Rawal, R., & Schnapp, S. (2015). Residential buildings in India: Energy use projections and savings potentials. *ECEEE SUMMER STUDY PROCEEDINGS*.
- Skoplaki, E., & Palyvos, J. A. (2009). On the temperature dependence of photovoltaic module electrical performance: A review of efficiency/power correlations. *Solar Energy*, 83(5), 614–624. <https://doi.org/https://doi.org/10.1016/j.solener.2008.10.008>
- Sobhnamayan, F., Sarhaddi, F., Alavi, M. A., Farahat, S., & Yazdanpanahi, J. (2014). Optimization of a solar photovoltaic thermal (PV/T) water collector based on exergy concept. *Renewable Energy*, 68, 356–365.
<https://doi.org/https://doi.org/10.1016/j.renene.2014.01.048>
- The World Bank. (2017). *India Transforms Market for Rooftop Solar*.
- Tiwari, A., & Sodha, M. S. (2007). Parametric study of various configurations of hybrid PV/thermal air collector: Experimental validation of theoretical model. *Solar Energy Materials and Solar Cells*, 91(1), 17–28.
<https://doi.org/https://doi.org/10.1016/j.solmat.2006.06.061>
- Tonui, J. K., & Tripanagnostopoulos, Y. (2007). Improved PV/T solar collectors with heat extraction by forced or natural air circulation. *Renewable Energy*, 32(4), 623–637.
<https://doi.org/https://doi.org/10.1016/j.renene.2006.03.006>
- Tripanagnostopoulos, Y., Nousia, T., Souliotis, M., & Yianoulis, P. (2002). Hybrid photovoltaic/thermal solar systems. *Solar Energy*, 72(3), 217–234.
[https://doi.org/https://doi.org/10.1016/S0038-092X\(01\)00096-2](https://doi.org/https://doi.org/10.1016/S0038-092X(01)00096-2)
- UN, S. (2017). *Rooftop solar is the fastest-growing segment in India's renewables market*.
- Yang, T., & Athienitis, A. K. (2014). A study of design options for a building integrated photovoltaic/thermal (BIPV/T) system with glazed air collector and multiple inlets. *Solar Energy*, 104, 82–92. <https://doi.org/https://doi.org/10.1016/j.solener.2014.01.049>
- Yang, T., & Athienitis, A. K. (2016). A review of research and developments of building-integrated photovoltaic/thermal (BIPV/T) systems. *Renewable and Sustainable Energy Reviews*, 66, 886–912. <https://doi.org/https://doi.org/10.1016/j.rser.2016.07.011>
- Zolpakar, N. A., Lodhi, S. S., Pathak, S., & Sharma, M. A. (2020). *Application of Multi-objective Genetic Algorithm (MOGA) Optimization in Machining Processes BT - Optimization of Manufacturing Processes* (K. Gupta & M. K. Gupta (eds.); pp. 185–199). Springer International Publishing. https://doi.org/10.1007/978-3-030-19638-7_8

Appendices

Appendix A

Based on this work, one conference paper has been published and one conference paper has been submitted:

1. **Nibandhe, A.**, Bonyadi, N., Rounis, E., Lee, B., Athienitis, A., & Bagchi, A. (2020). Design of a coupled BIPV/T - Solid desiccant cooling system for a warm and humid climate. *Proceedings of the ISES Solar World Congress 2019 and IEA SHC International Conference on Solar Heating and Cooling for Buildings and Industry, Santiago, Chile 2019*. <https://doi.org/10.18086/swc.2019.55.10>
2. Bonyadi, N., **Nibandhe, A.**, Rounis.,E, Lee, B., Athienitis, A., & Bagchi, A. (2021). Multi-objective Optimization of a Coupled BIPV/T-Solid Desiccant Cooling System for a Warm and Humid Climate. *Proceedings of the eSIM Conference, Vancouver, Canada.2021. (Submitted)*.

Appendix B

Table 15 presents the electricity consumption data (2009) for 417 residential units from 6 residential complexes in Chennai, India. For the purpose of comparison, the residential unit area has to be same. Therefore, based on the available surveyed data, energy consumption data for residential unit area of 55 m² is calculated and compared with the simulated data.

It is often the case in India that buildings are either fully, partially conditioned or not conditioned at all. Therefore, Energy Performance Index (EPI)(kWh/m².year) is a commonly used performance indicator for buildings in India. EPI is defined as the energy consumed per total floor area (not considering the common areas and parking space).

Figure 31 illustrates the comparison of the surveyed data and simulated data. The low-rise mixed-used building in this study comprises of 12 residential units (for example U_11 for unit number 1 on the first floor and so on). The EPI of the residential units from simulated data are within acceptable range of the EPI available from the surveyed data.

Parameter	Surveyed data	Projected data	Simulated data
Built-up area (m ²)	50 – 220	55	55
Avg. annual consumption (kWh)	4,050	3,192	3,288
Building envelope	Assumed same		
No. of occupants	Assumed same		
EPI (kWh/m ² .year)	44	60	60 – 70

Table 15 Comparison of Surveyed Data and Simulated Data

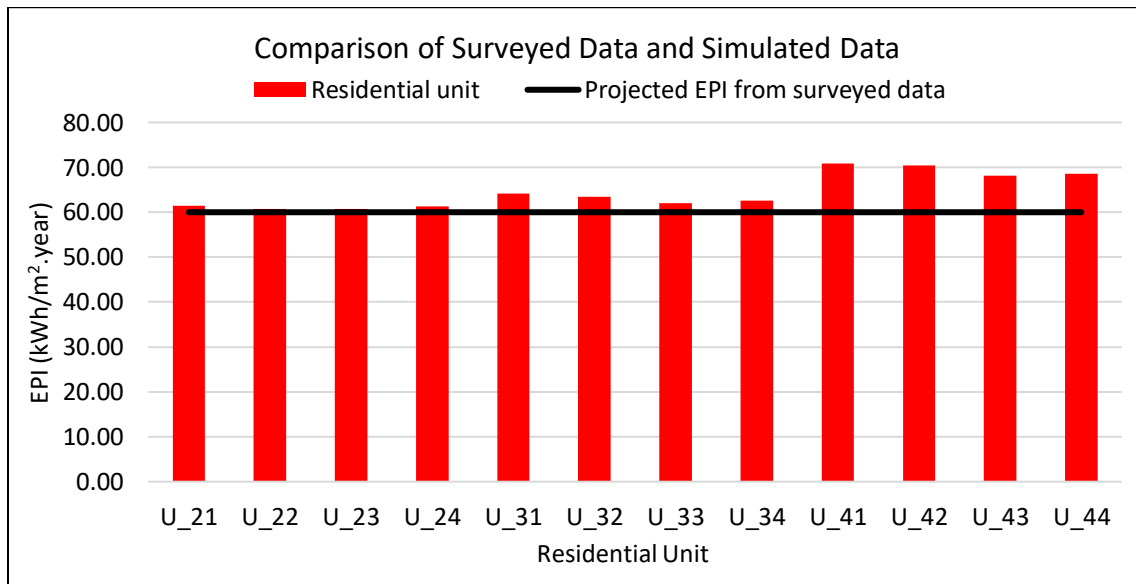


Figure 31 Comparison of Surveyed Data and Simulated Data

Appendix C

This section presents the steady state operation of the integrated system configurations using psychrometric chart. The steady state conditions are taken for June 1st at 12 pm.

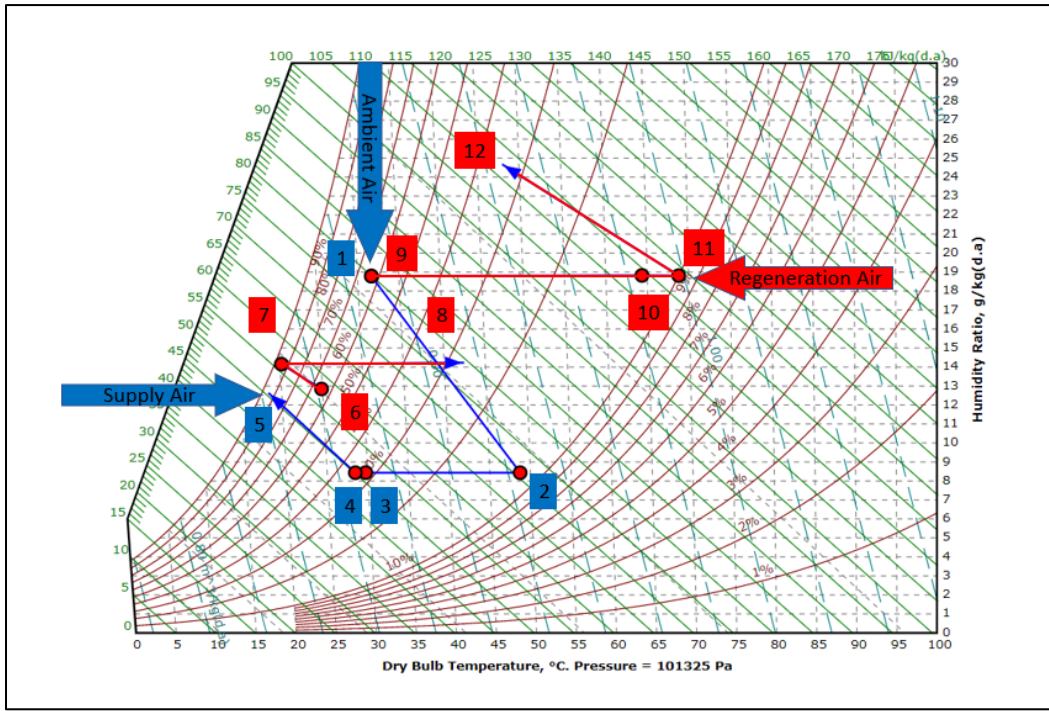


Figure 32 Psychrometric chart showing steady state operation of integrated system configuration 1 (Flycarpet, 2020)

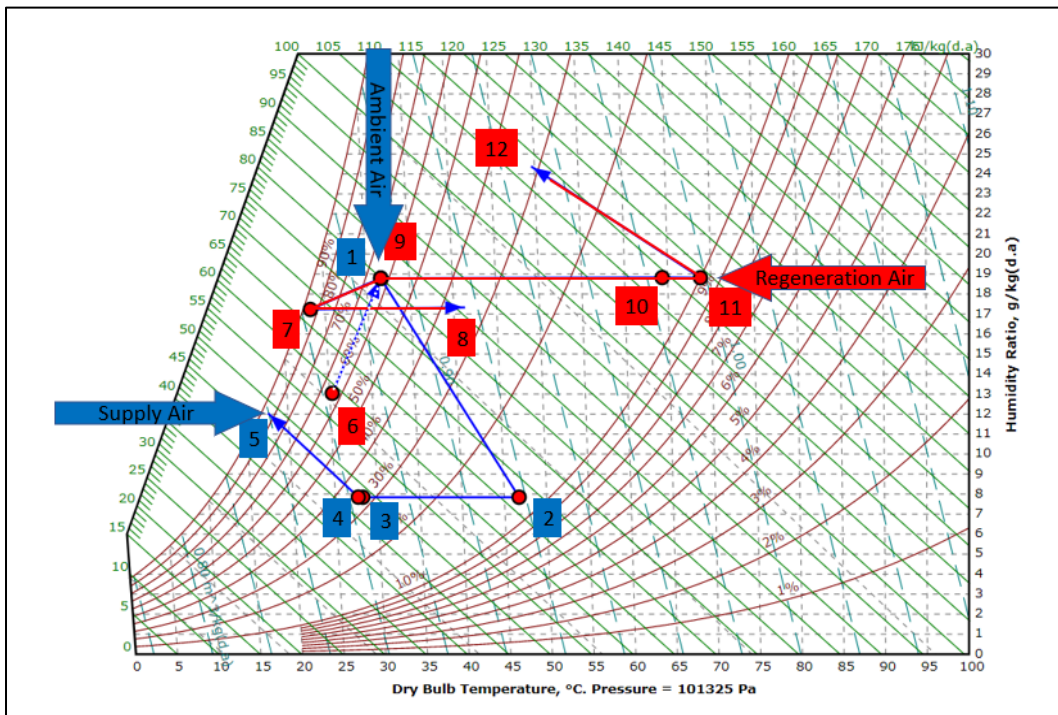


Figure 33 Psychrometric chart showing steady state operation of integrated system configuration 2 (Flycarpet, 2020)

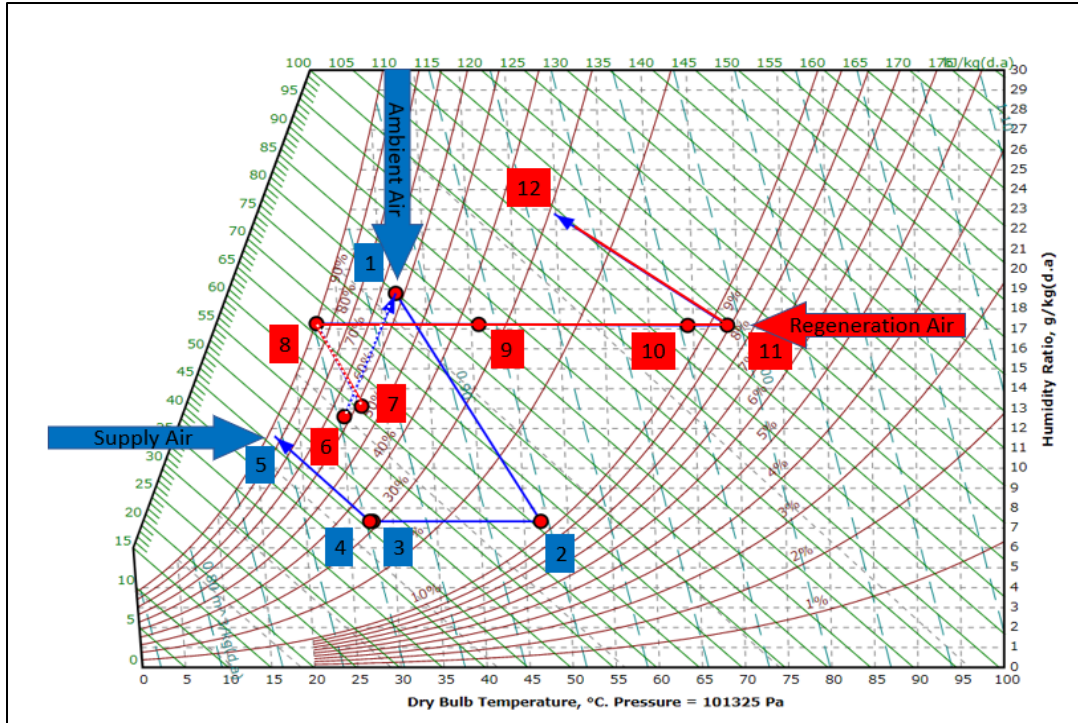


Figure 34 Psychrometric chart showing steady state operation of integrated system configuration 3 (Flycarpet, 2020)

Appendix D

Parallel plots illustrating all the different designs are presented here.

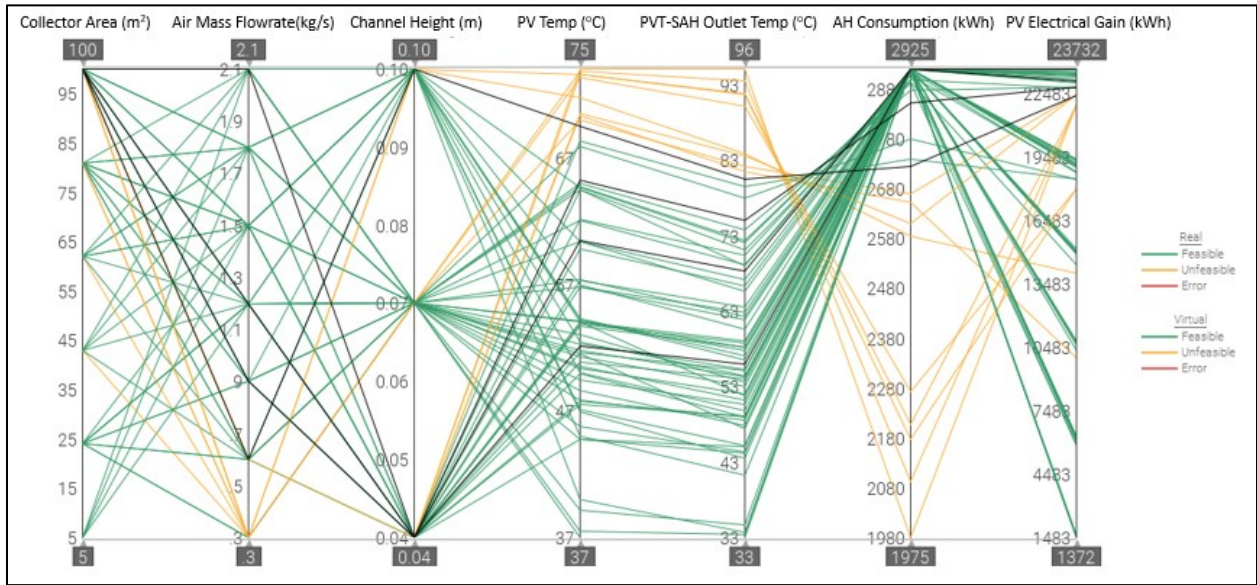


Figure 35 Parallel Plot with all possible integrated system designs

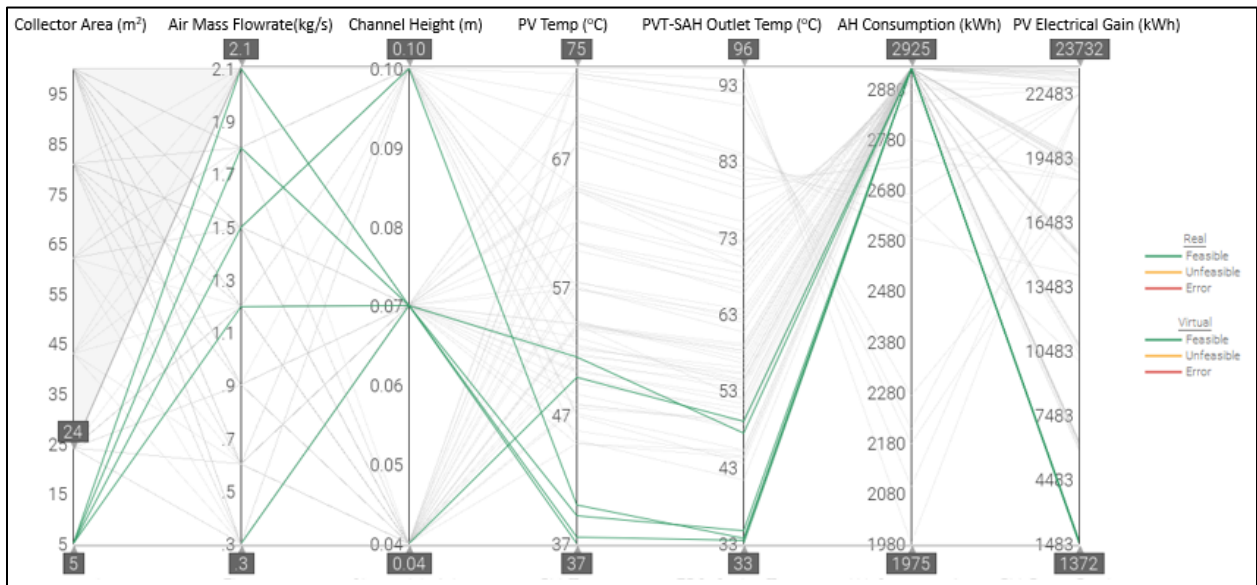


Figure 36 Parallel Plot showing variation in outputs for small collector areas

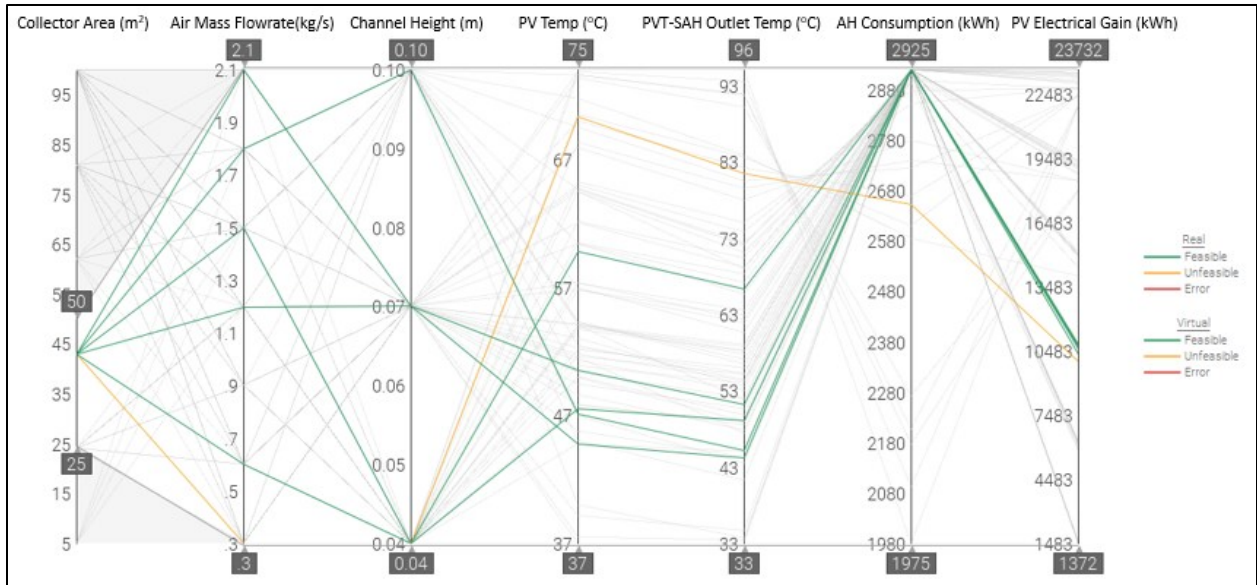


Figure 37 Parallel Plot showing variation in outputs for medium collector areas

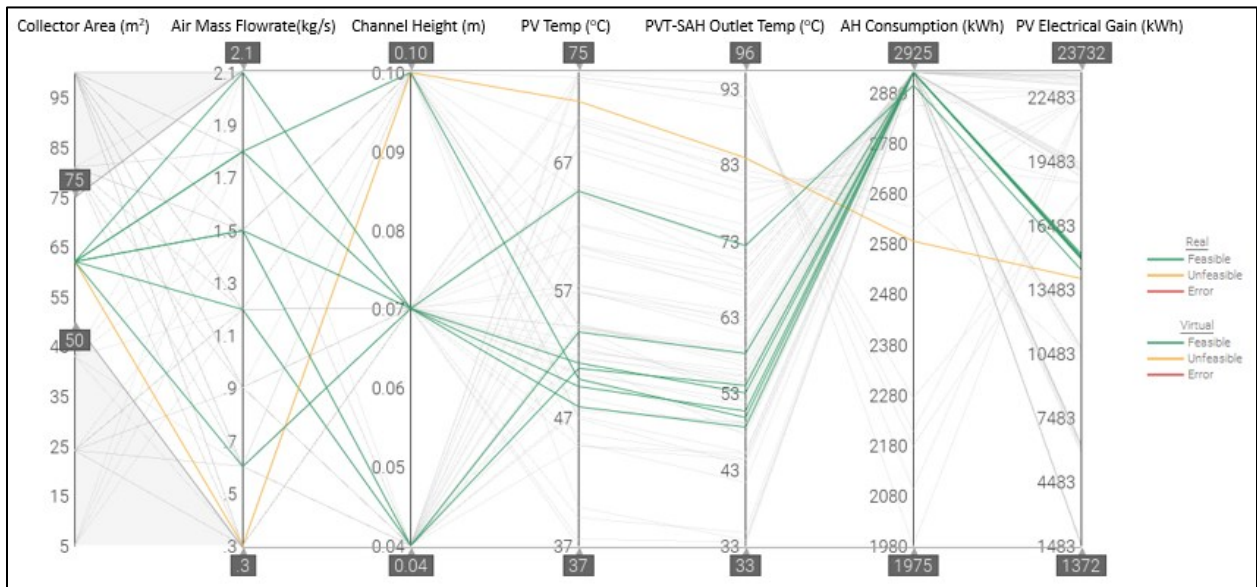


Figure 38 Parallel Plot showing variation in outputs for medium collector areas

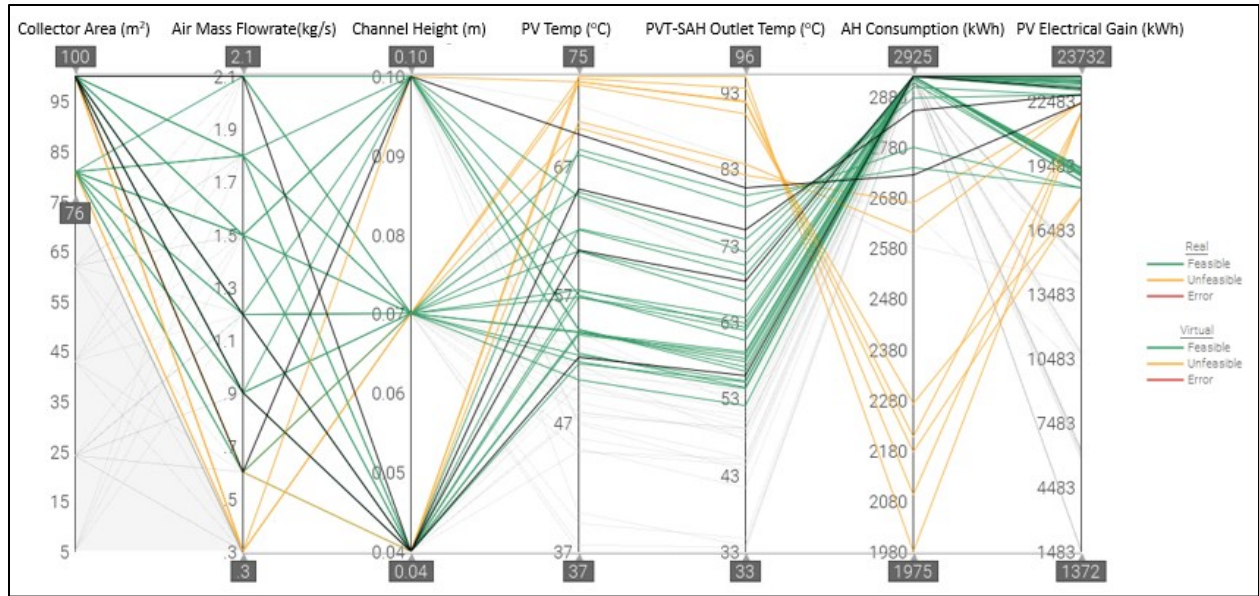


Figure 39 Parallel Plot showing variation in outputs for large collector areas